

Ultrafast Nonlinear X-ray Spectroscopy of Molecules: Theoretical Challenges

Shaul Mukamel and Satoshi Tanaka
University of Rochester

Principles of Nonlinear Optical Spectroscopy, S. Mukamel, (Oxford University Press, New York) (1995).

“Time-Resolved X-Ray Spectroscopies; Nonlinear Response Functions and Liouville-Space Pathways,” S. Tanaka, V. Chernyak and S. Mukamel, *Phys. Rev. A*. **63**, 63405-63419 (2001).

“Simulation of Frequency and Wavevector resolved femtosecond resonant x-ray emission of molecular chains,” S. Tanaka and S. Mukamel, *Phys. Rev. A*. **64**, 032503/1-13 (2001).

“X-Ray Four-Wave Mixing in Molecules,” S. Tanaka and S. Mukamel, *J. Chem. Phys.* **116**, 1877-1891 (2002).

“Coherent X-Ray Raman Spectroscopy,” S. Tanaka and S. Mukamel, *Phys. Rev. Lett.* (Submitted) (2001).

1. Background

- Recent progress in experimental techniques

ultrafast attosecond x-ray pulses
intense x-ray beams

high harmonics of optical laser pulses
third-generation-synchrotron radiation

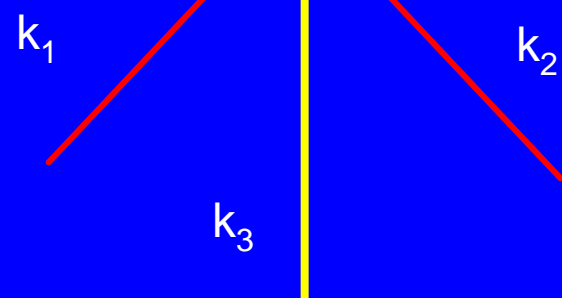
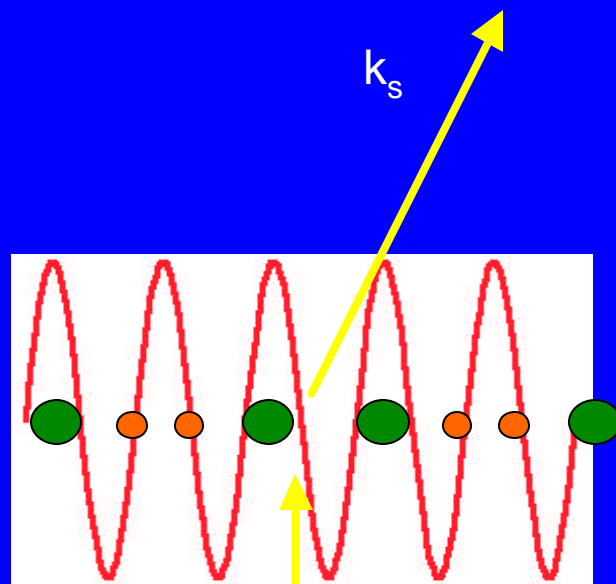
→ Ultrafast nonlinear x-ray spectroscopy

Ultrafast electron dynamics

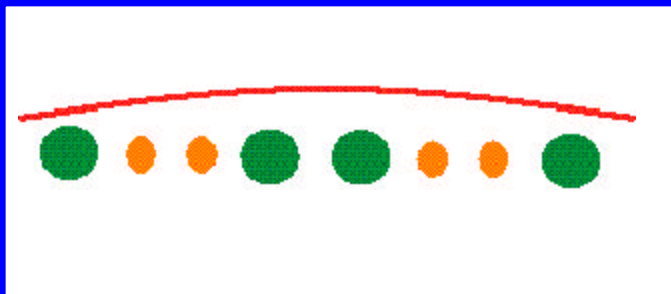
In real-time, real-space

2) Spatial resolution

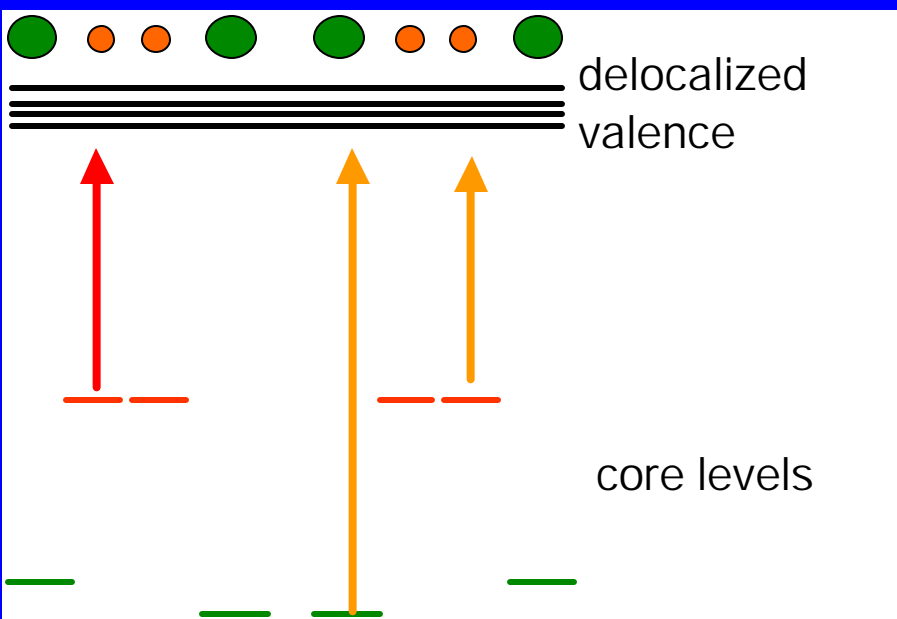
X-ray: spatial coherence



Atomic scale transient grating



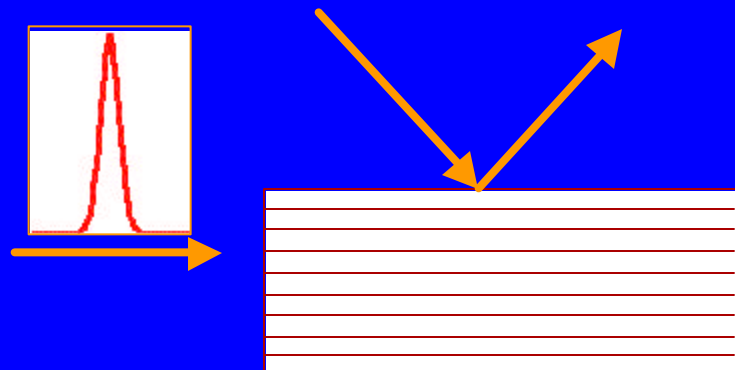
Optical light:
Spatial information is averaged out
(Long wavelength limit)



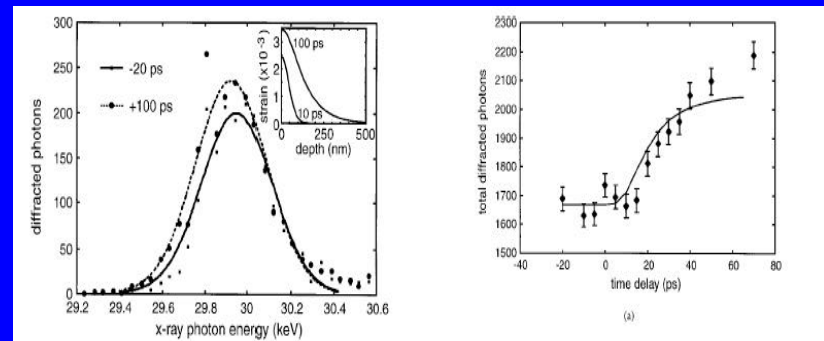
Site selectivity by core resonance

4. Experiments of time-resolved x-ray spectroscopy

- Time-resolved X-ray diffraction

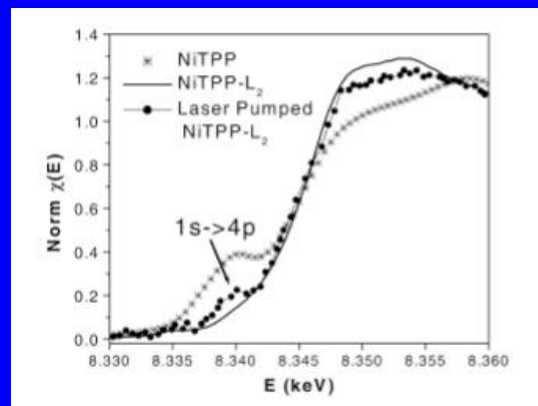
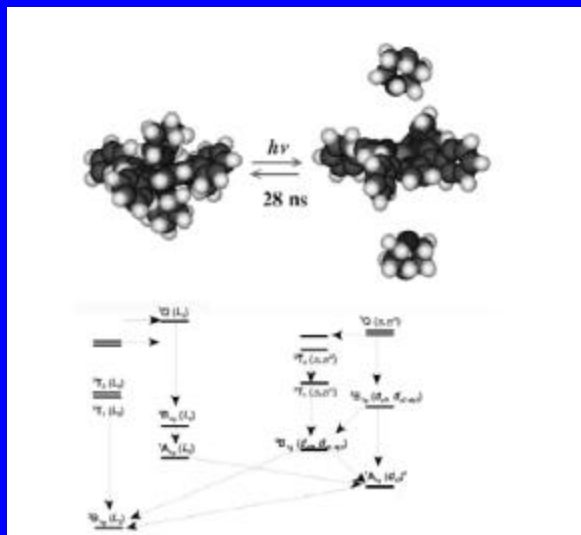


Temporal change of lattice constant of InSb after intense laser excitation, Chin, PRL83,336(99)



- Time-resolved X-ray absorption(XANES and EXAFS)

Temporal change of local structure around Ni metal in Ni porphyrin

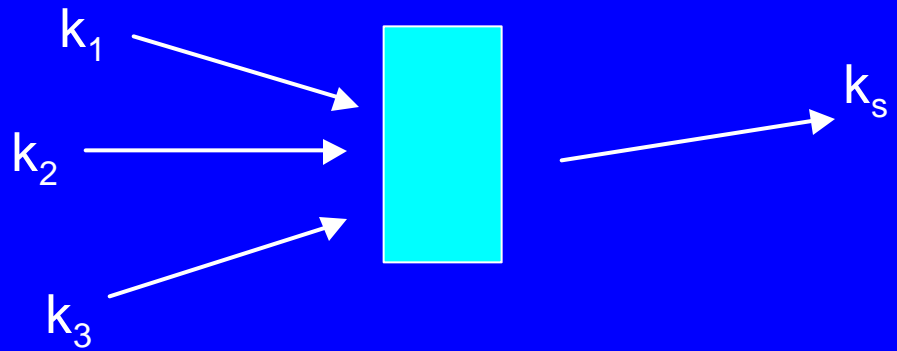


Ni 1s edge time-resolved EXAFS
L.X.Chen,J.E.S.R.P.119,161(01)

Outline

- 1) develop general theoretical approach for nonlinear x-ray spectroscopy,
drawing upon the analogy with nonlinear optics

- 2) simulation of nonlinear x-ray spectra
 - i. Time-resolved x-ray emission
 - ii. x-ray pump-probe spectra in nitroanilines
 - iii. coherent x-ray Raman scattering
 - iv. Time-resolved coherent x-ray Raman spectroscopy



Goals

- x-ray wavelength ($1\text{\AA}\sim 100\text{\AA}$) ? molecular size
 - Microscopic nonlocal effects
- breakdown of dipole approximation
 - Minimal coupling Hamiltonian
- unified description for various nonlinear x-ray and optical techniques
 - Nonlinear response function in Liouville space

- Minimal coupling Hamiltonian

$$H = H_{mat} + H_{int},$$

$$H_{int} = H_1 + H_2,$$

$$H_1 = - \int \mathbf{A}(\mathbf{r}, t) \cdot \hat{\mathbf{j}}(\mathbf{r}) d\mathbf{r},$$

$$H_2 = \frac{e^2}{2mc} \int \mathbf{A}^2(\mathbf{r}, t) \hat{\sigma}(\mathbf{r}) d\mathbf{r}.$$

$$\hat{\mathbf{j}}(\mathbf{r}) \equiv \frac{e\hbar}{2mi} \{ \hat{\psi}^\dagger(\mathbf{r}) \nabla \hat{\psi}(\mathbf{r}) - [\nabla \hat{\psi}(\mathbf{r})^\dagger] \hat{\psi}(\mathbf{r}) \},$$

$$\hat{\sigma}(\mathbf{r}) \equiv \hat{\psi}^\dagger(\mathbf{r}) \hat{\psi}(\mathbf{r}),$$

- Quantum Liouville equation

$$i\hbar \frac{d}{dt} \mathbf{r}(t) = [H(t), \mathbf{r}(t)]$$

- Expectation value of current density

$$\begin{aligned} \mathbf{J}(\mathbf{r}, t) &= \langle \hat{\mathbf{j}}(\mathbf{r}) \rangle_t - \frac{e^2}{2mc} \mathbf{A}(\mathbf{r}, t) \langle \hat{\sigma}(\mathbf{r}) \rangle_t, \\ &= \text{Tr}[\hat{\mathbf{j}}(\mathbf{r}) \rho(t)] - \frac{e^2}{2mc} \mathbf{A}(\mathbf{r}, t) \text{Tr}[\hat{\sigma}(\mathbf{r}) \rho(t)], \end{aligned}$$

- Perturbative expansion of the density matrix $\rho(t)$ in the radiation field $A(r,t)$

$$\rho(t) = \rho^{(0)}(t) + \rho^{(1)}(t) + \dots,$$

- Expectation value of current density expanded in powers of the field

$$J_{\lambda_s}^{(n)}(\mathbf{r},t) = \int d\mathbf{r}_n \int d\mathbf{r}_{n-1} \cdots \int d\mathbf{r}_1 \int dt_n \int dt_{n-1} \cdots \int dt_1 \\ \times \sum_{\lambda_1, \dots, \lambda_n} \underbrace{\mathbb{S}_{\lambda_n, \dots, \lambda_1 \lambda_s}^{(n)}(\mathbf{r}; \mathbf{r}_n, \mathbf{r}_{n-1}, \dots, t_n, t_{n-1}, \dots, t_1)}_{\text{Nonlinear response function}} A_{\lambda_n}(\mathbf{r}_n, t - t_n) \\ \times A_{\lambda_{n-1}}(\mathbf{r}_{n-1}, t - t_n - t_{n-1}) \times \cdots \times A_{\lambda_1}(\mathbf{r}_1, t - t_n - t_{n-1} - \cdots - t_1).$$

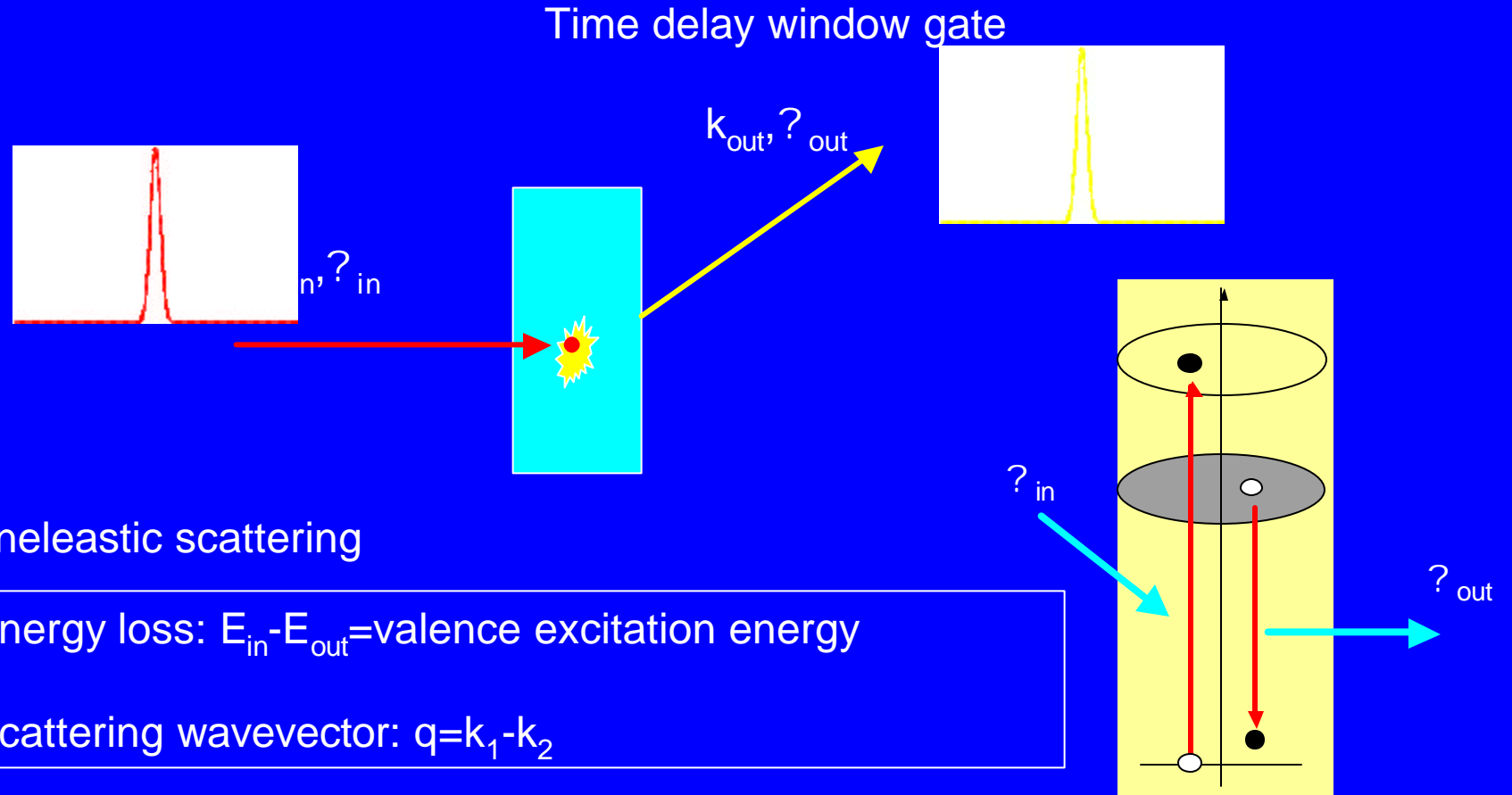
Nonlinear response function

Nonlocal effects are built in

- 3rd-order nonlinear response function

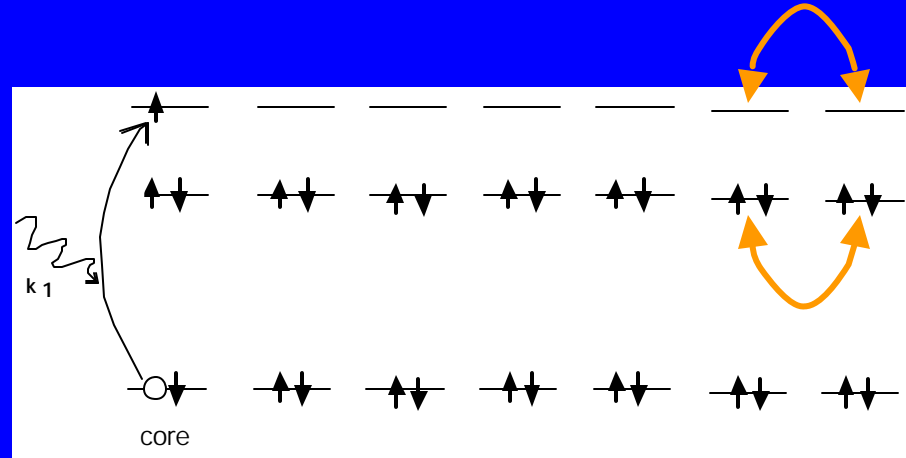
$$\begin{aligned}
S_{\lambda_3 \lambda_2 \lambda_1 \lambda_s}^{(3)}(\mathbf{r}; \mathbf{r}_3 \mathbf{r}_2 \mathbf{r}_1 t_3 t_2 t_1) = & (-) \left(-\frac{i}{\hbar} \right)^3 \langle \langle \hat{j}_{\lambda_s}(\mathbf{r}) | \mathcal{G}(t_3) \mathcal{J}_{0\lambda_3}(\mathbf{r}_3) \mathcal{G}(t_2) \mathcal{J}_{0\lambda_2}(\mathbf{r}_2) \mathcal{G}(t_1) \mathcal{T}_{0\lambda_1}(\mathbf{r}_1) | \rho(-\infty) \rangle \rangle \\
& + \left(-\frac{e^2}{2mc} \right) \left(-\frac{i}{\hbar} \right)^2 \{ \langle \langle \hat{j}_{\lambda_s}(\mathbf{r}) | \mathcal{G}(t_3) \mathcal{Z}(\mathbf{r}_3) \mathcal{G}(t_1) \mathcal{J}_{0\lambda_1}(\mathbf{r}_1) | \rho(-\infty) \rangle \rangle \delta_{\lambda_2 \lambda_3} \delta(\mathbf{r}_2 - \mathbf{r}_3) \delta(t_2) \\
& + \langle \langle \hat{j}_{\lambda_s}(\mathbf{r}) | \mathcal{G}(t_3) \mathcal{J}_{0\lambda_3}(\mathbf{r}_3) \mathcal{G}(t_2) \mathcal{Z}(\mathbf{r}_2) | \rho(-\infty) \rangle \rangle \delta_{\lambda_2 \lambda_1} \delta(\mathbf{r}_2 - \mathbf{r}_1) \delta(t_1) \\
& + \langle \langle \hat{\sigma}(\mathbf{r}) | \mathcal{G}(t_2) \mathcal{J}_{0\lambda_2}(\mathbf{r}_2) \mathcal{G}(t_1) \mathcal{J}_{0\lambda_1}(\mathbf{r}_1) | \rho(-\infty) \rangle \rangle \delta_{\lambda_3 \lambda_s} \delta(\mathbf{r} - \mathbf{r}_3) \delta(t_3) \} - \left(\frac{e^2}{2mc} \right)^2 \left(-\frac{i}{\hbar} \right) \\
& \times \langle \langle \hat{\sigma}(\mathbf{r}) | \mathcal{G}(t_2) \mathcal{Z}(\mathbf{r}_2) | \rho(-\infty) \rangle \rangle \delta_{\lambda_3 \lambda_s} \delta_{\lambda_2 \lambda_1} \delta(\mathbf{r} - \mathbf{r}_3) \delta(\mathbf{r}_2 - \mathbf{r}_1) \delta(t_3) \delta(t_1).
\end{aligned}$$

7. Time- and frequency resolved X-ray emission spectrum (TFXES)

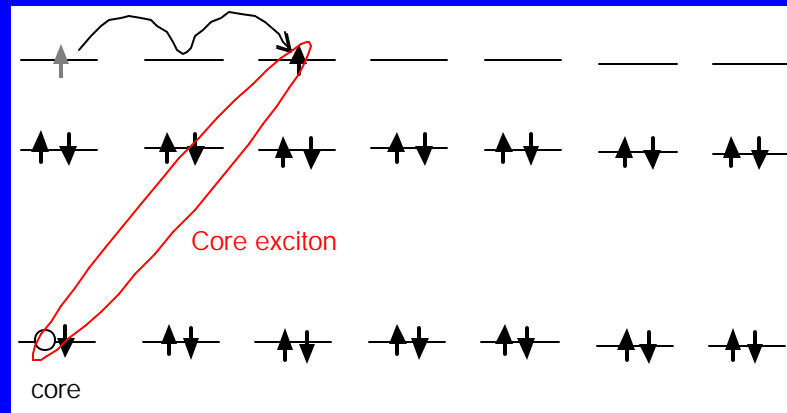


Detection of entire band of valence excitation : $(q, ?)$
(not only $q=0$ but also $q \neq 0$)

excitation



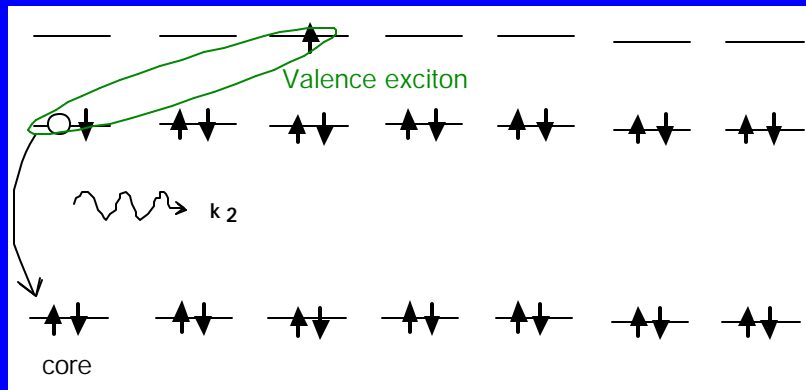
migration



Core hole transfer= 0

X-ray excitation and
emission take place at the
same site

emission



- Hamiltonian:
tight-binding + Coulomb(core-conduction & valence-conduction)

$$\begin{aligned}
H = & - \sum_{l=0}^{N-1} \mathbf{e}_{core} a_l^\dagger a_l + \sum_{l=0}^{N-1} \mathbf{e}_{val} v_l^\dagger v_l - \sum_{l=0}^{N-1} \mathbf{e}_{cond} c_l^\dagger c_l \\
& + \sum_{l,m=0}^{N-1} t_{lm}^{val} v_l^\dagger v_m + \sum_{l,m=0}^{N-1} t_{lm}^{cond} c_l^\dagger c_m \\
& - \sum_{l,l',m,m'} U_{l'm';lm}^{core-cond} c_{l'}^\dagger a_{m'}^\dagger a_m c_l - \sum_{l,l',m,m'} U_{l'm';lm}^{val-cond} c_{l'}^\dagger v_{m'}^\dagger v_m c_l
\end{aligned}$$

Core exciton

Valence exciton

site energy

transfer energy

Coulomb

- Direct diagonalization:
basis set

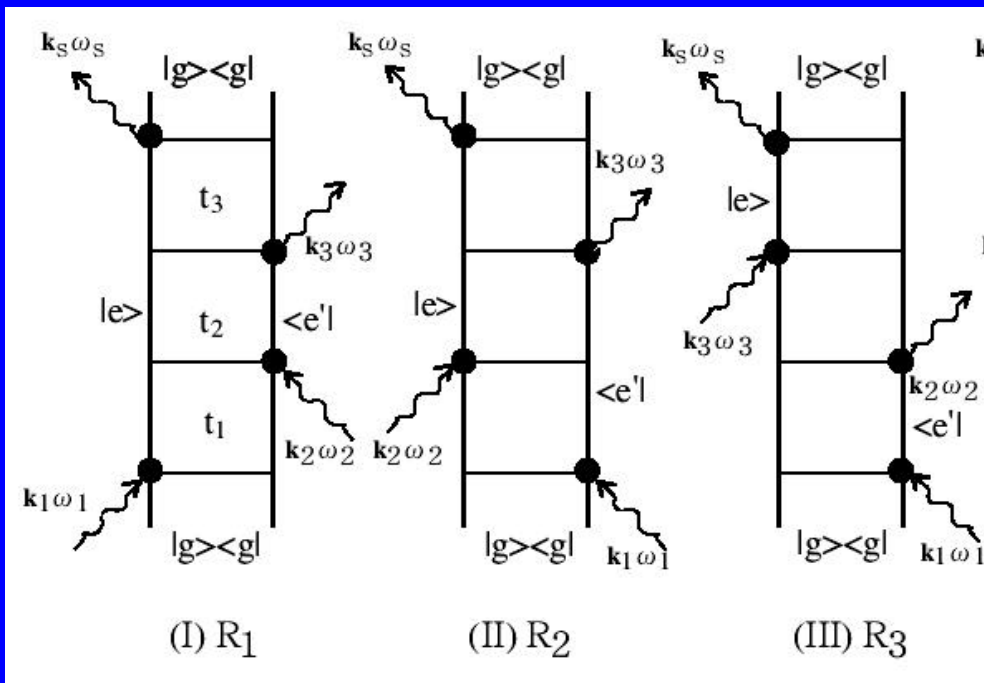
$$| l_{core} m_{cond} \rangle = a_l^\dagger c_m^\dagger | g \rangle$$

Core excited state

$$| l_{val} m_{cond} \rangle = v_l^\dagger c_m^\dagger | g \rangle$$

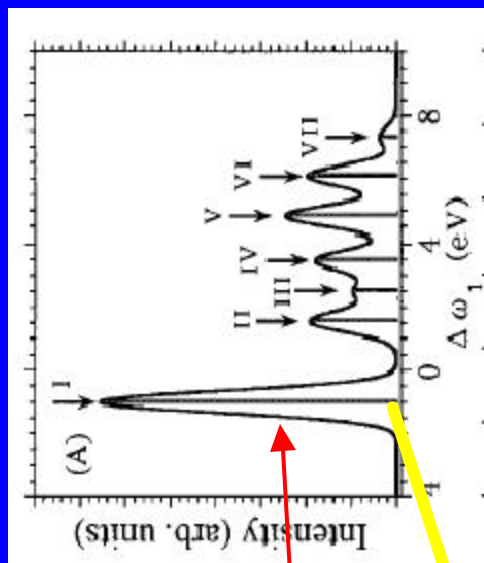
Valence excited state

$$\begin{aligned}
F(\mathbf{k}_1, \mathbf{k}_2; \tau) = & 2 \operatorname{Re} \sum_{l_1 l_2 l_3} \int_{-\infty}^{\infty} dt \int_0^{\infty} dt_3 \int_0^{\infty} dt_2 \int_0^{\infty} dt_1 \{ A_1(t + \tau - t_1 - t_2 - t_3) A_1^*(t + \tau - t_2 - t_3) A_t(t - t_3) A_t^*(t) \\
& \times \exp[i\omega_1 t_1 + i\omega_2 t_3] \exp[i\mathbf{k}_1 \cdot (\mathbf{R}_{l_1} - \mathbf{R}_{l_2})] \exp[i\mathbf{k}_2 \cdot (\mathbf{R}_{l_3} - \mathbf{R}_t)] R_1(l; l_3 l_2 l_1 t_3 t_2 t_1) \\
& + A_1^*(t + \tau - t_1 - t_2 - t_3) A_1(t + \tau - t_2 - t_3) A_t(t - t_3) A_t^*(t) \exp[-i\omega_1 t_1 + i\omega_2 t_3] \exp[-i\mathbf{k}_1 \cdot (\mathbf{R}_{l_1} - \mathbf{R}_{l_2})] \\
& \times \exp[-i\mathbf{k}_2 \cdot (\mathbf{R}_t - \mathbf{R}_{l_3})] R_2(l; l_3 l_2 l_1 t_3 t_2 t_1) + A_1^*(t + \tau - t_1 - t_2 - t_3) A_1(t + \tau - t_3) A_t(t - t_2 - t_3) A_t^*(t) \\
& \times \exp[-i\omega_1 t_1 - i(\omega_1 - \omega_2) t_2 + i\omega_2 t_3] \exp[-i\mathbf{k}_1 \cdot (\mathbf{R}_{l_1} - \mathbf{R}_{l_3})] \exp[-i\mathbf{k}_2 \cdot (\mathbf{R}_t - \mathbf{R}_{l_2})] R_3(l; l_3 l_2 l_1 t_3 t_2 t_1) \}.
\end{aligned}$$



$$\begin{aligned}
r_{a,b}(t) &\equiv \langle a | r(t) | b \rangle \\
&= \langle a | \Psi(t) \rangle \langle \Psi(t) | b \rangle
\end{aligned}$$

- Transition process



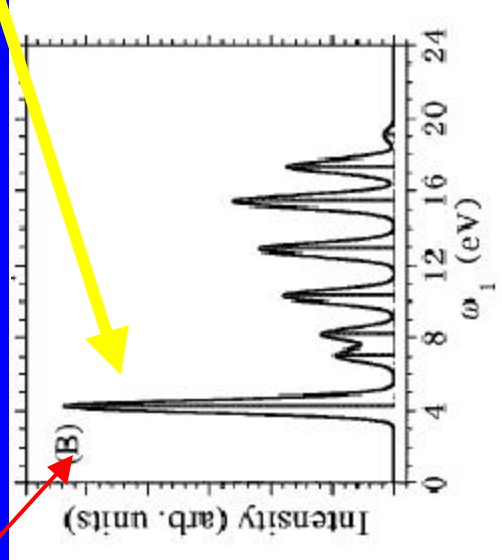
Delocalized Core excited states

Localized core exciton

X-ray emission

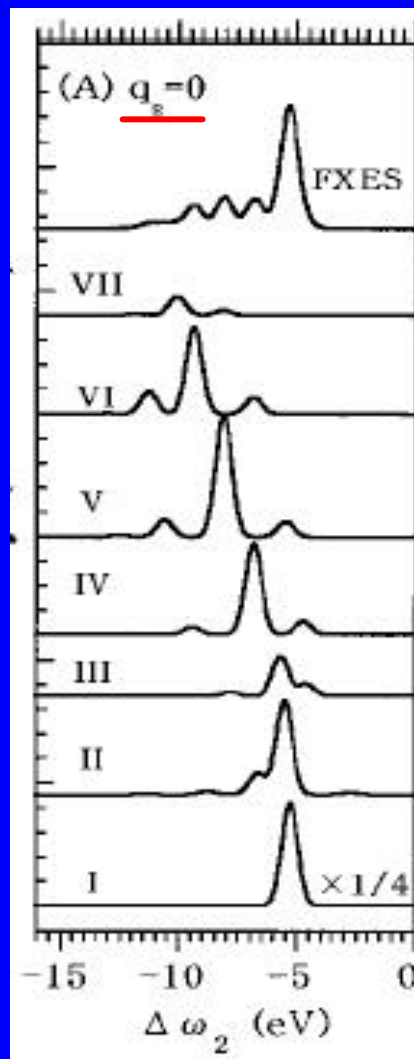
X-ray absorption

$|G\rangle$

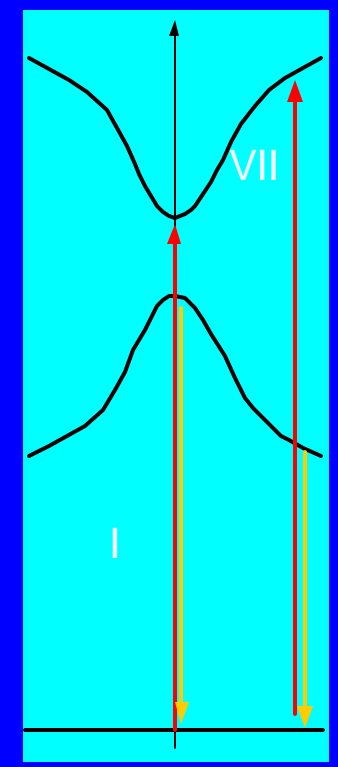


Optical absorption

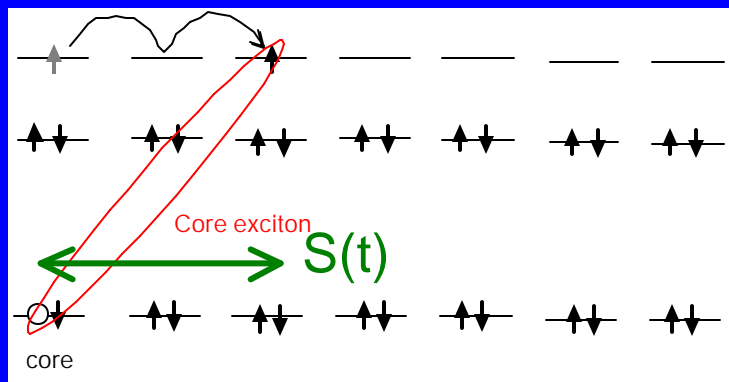
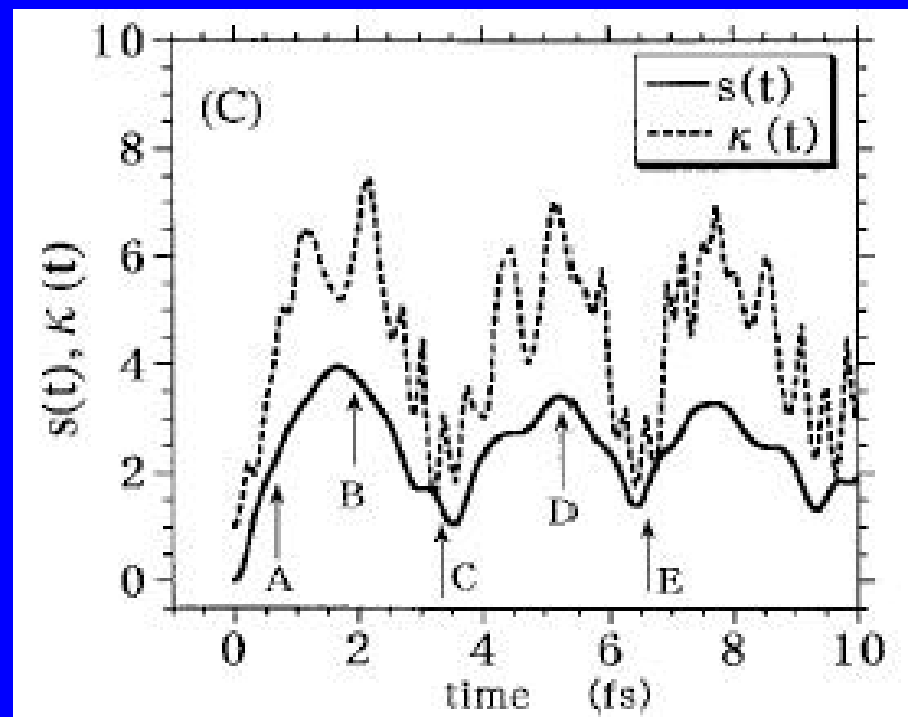
Stationary x-ray emission spectrum



Valence exciton states



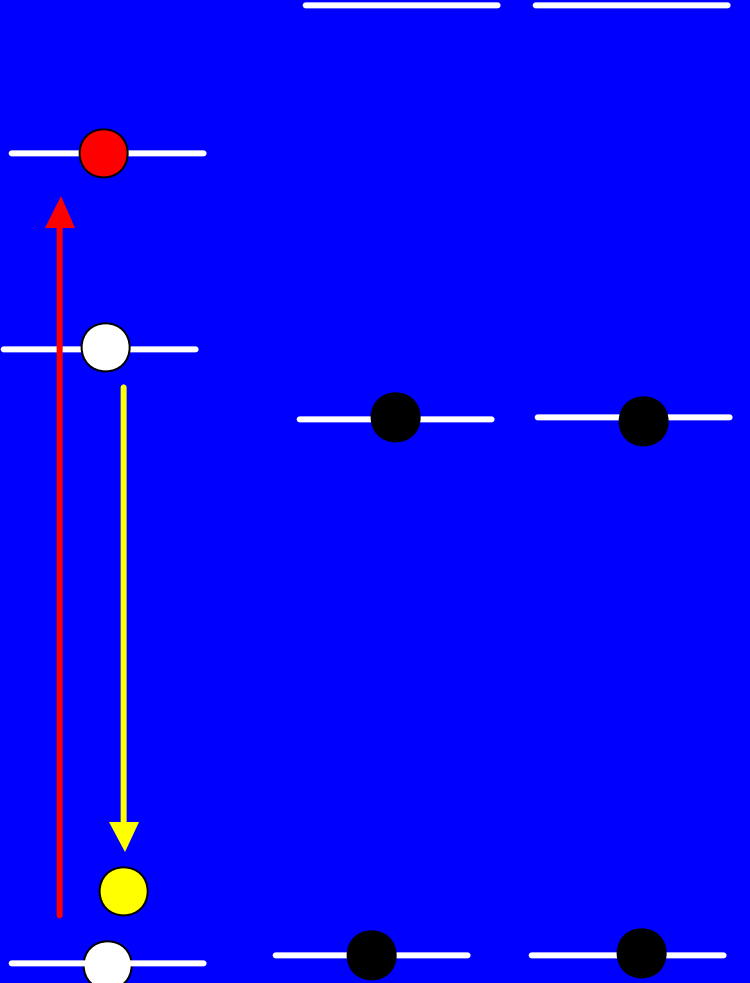
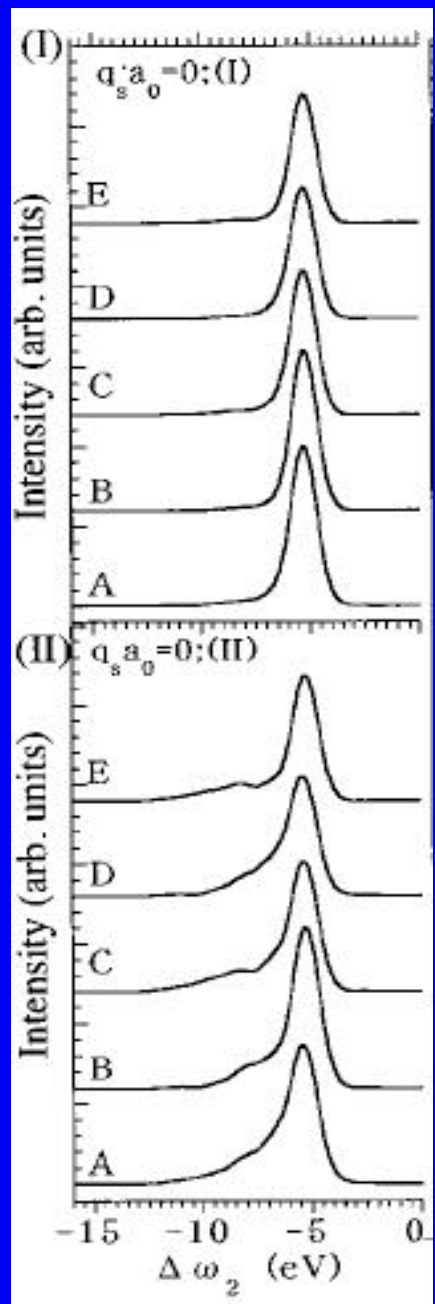
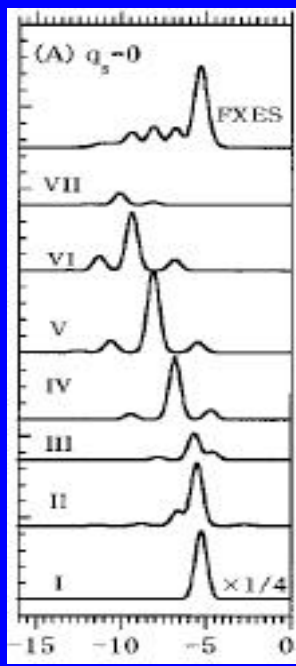
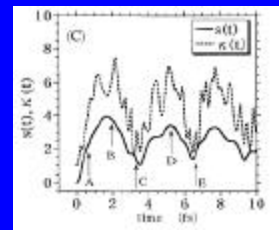
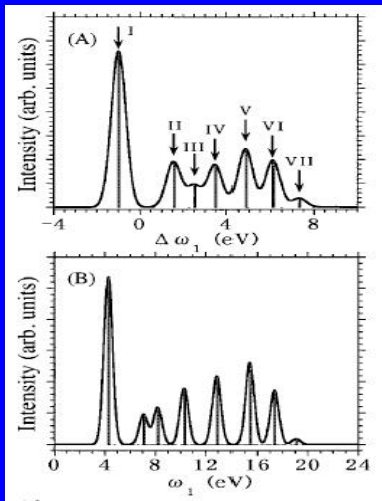
Time evolution of core exciton
 $S(t)$ average electron-hole separation
 $K(t)$ - width of the exciton wave function
(Inverse participation ratio)

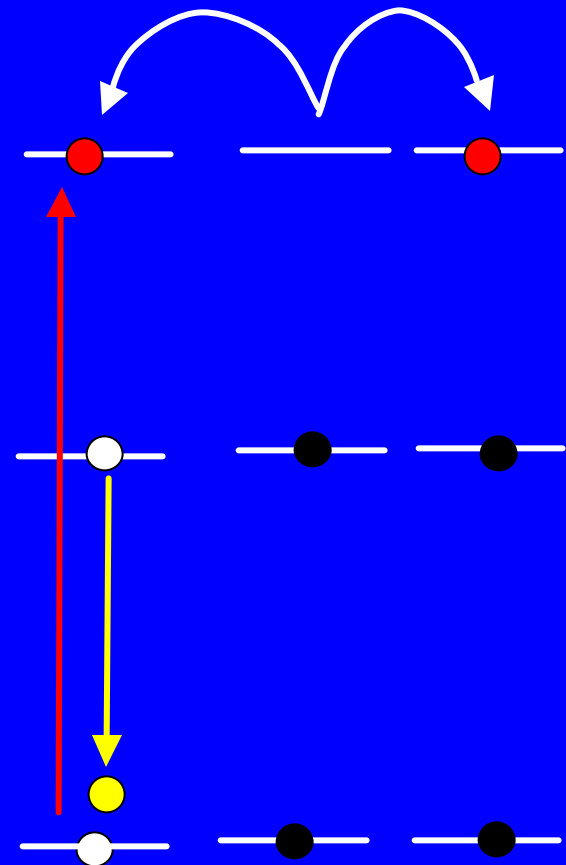
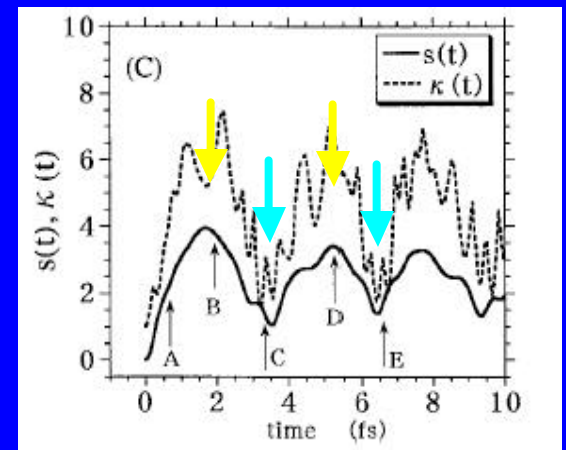
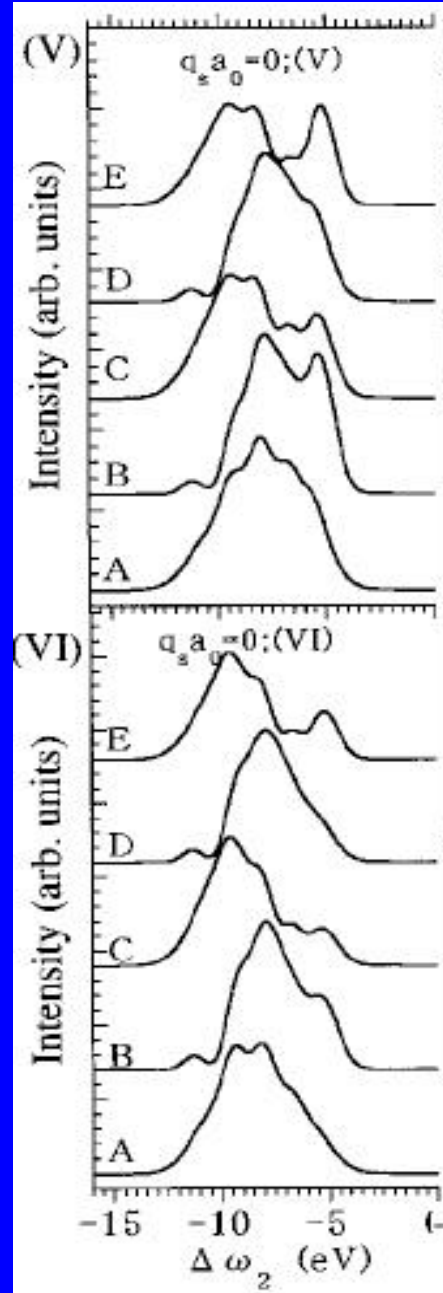
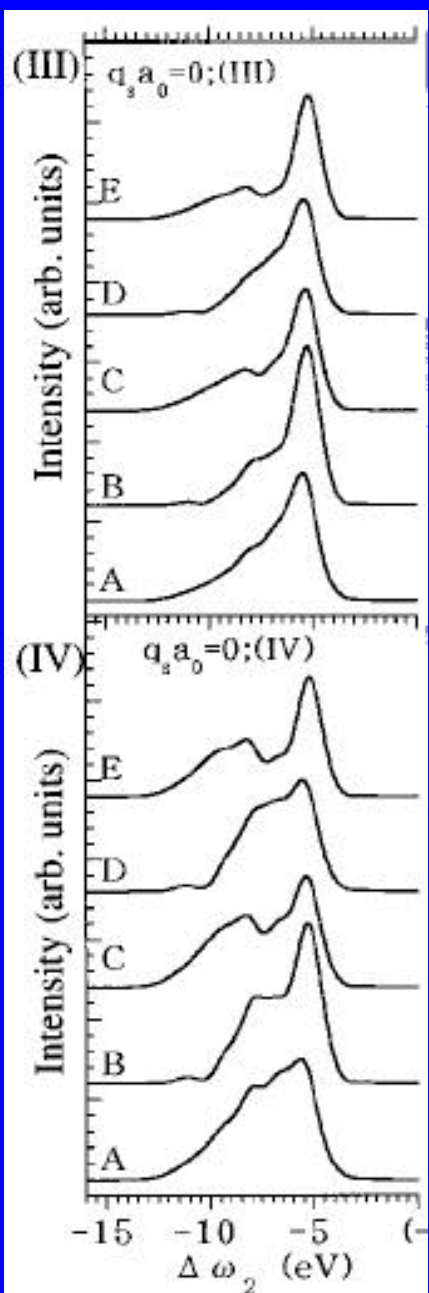


$$s(t) = \sum_j j P_j(t)$$

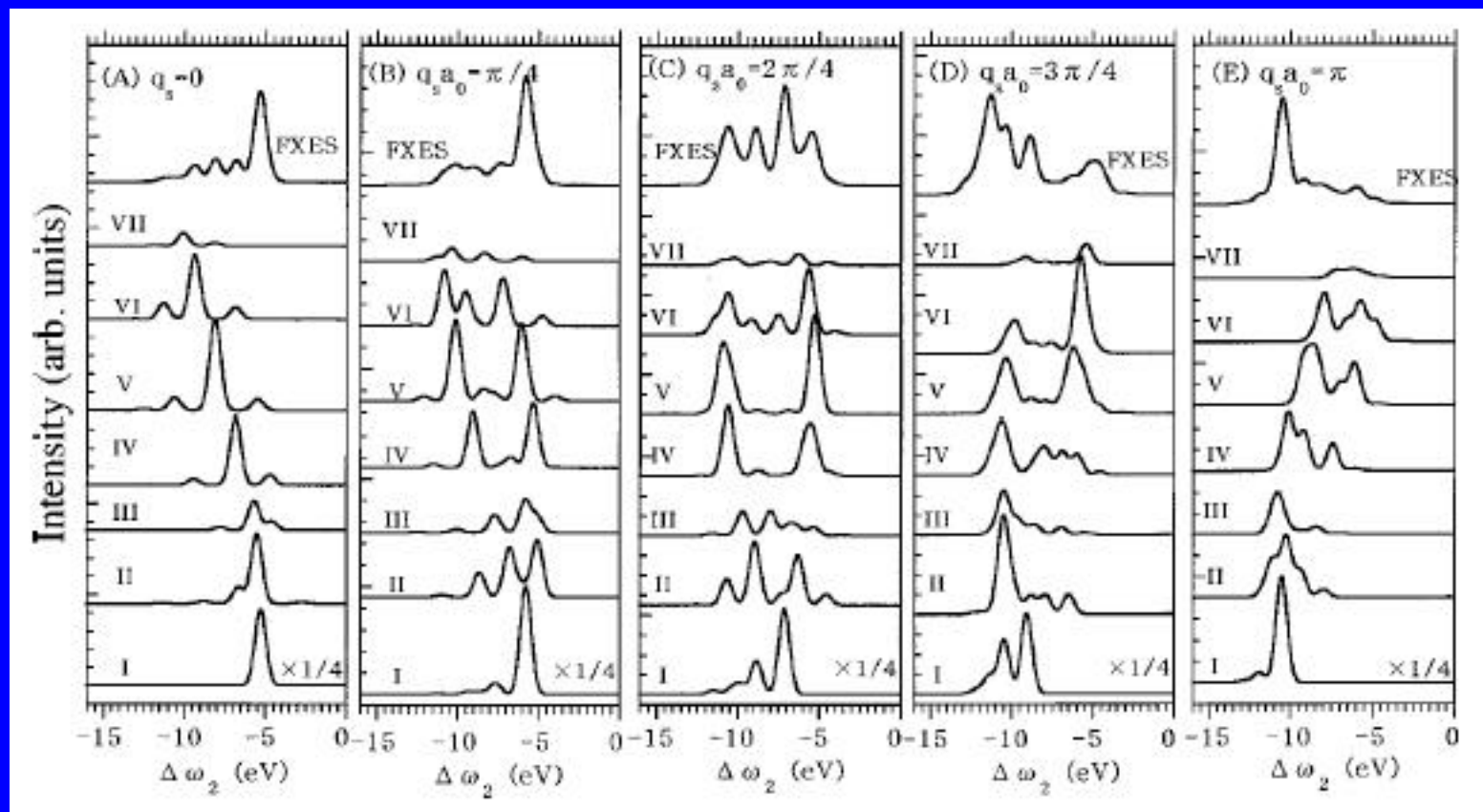
$$P_j(t) = \left| \langle l_{core}, l + j | \Psi(t) \rangle \right|^2$$

$$K(t) = \sqrt{\sum_j P_j^2(t)}$$





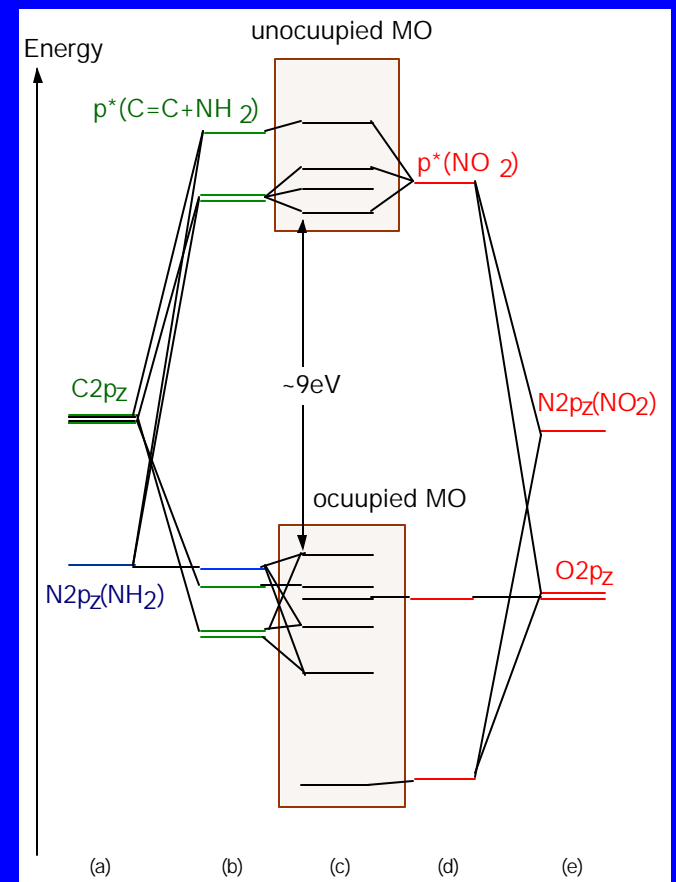
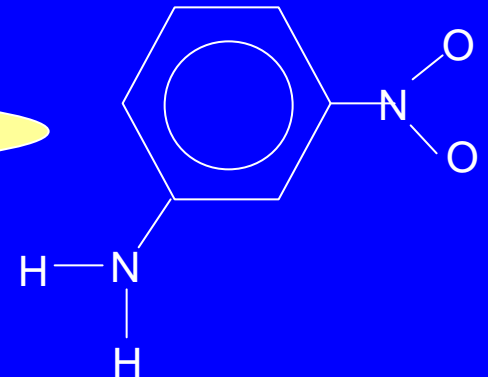
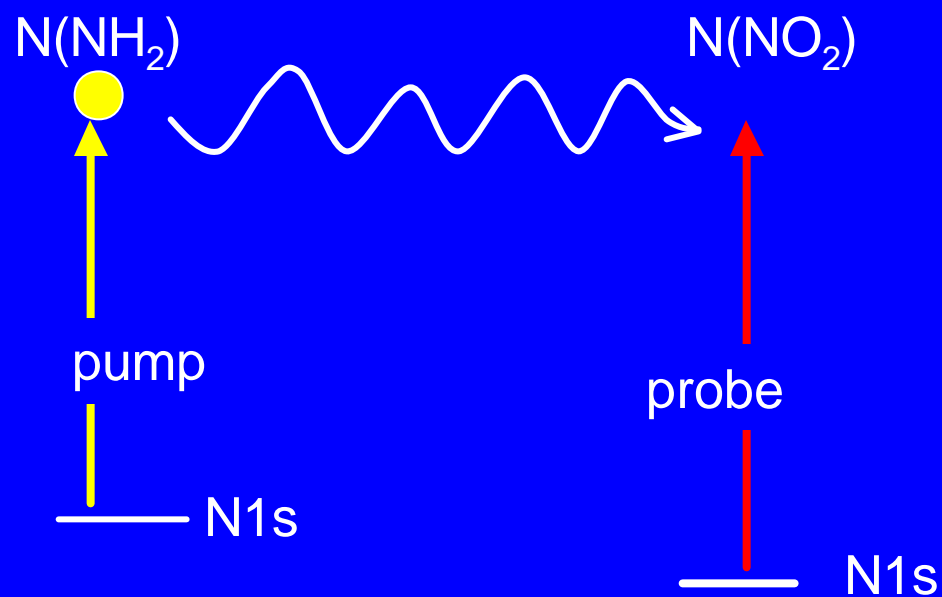
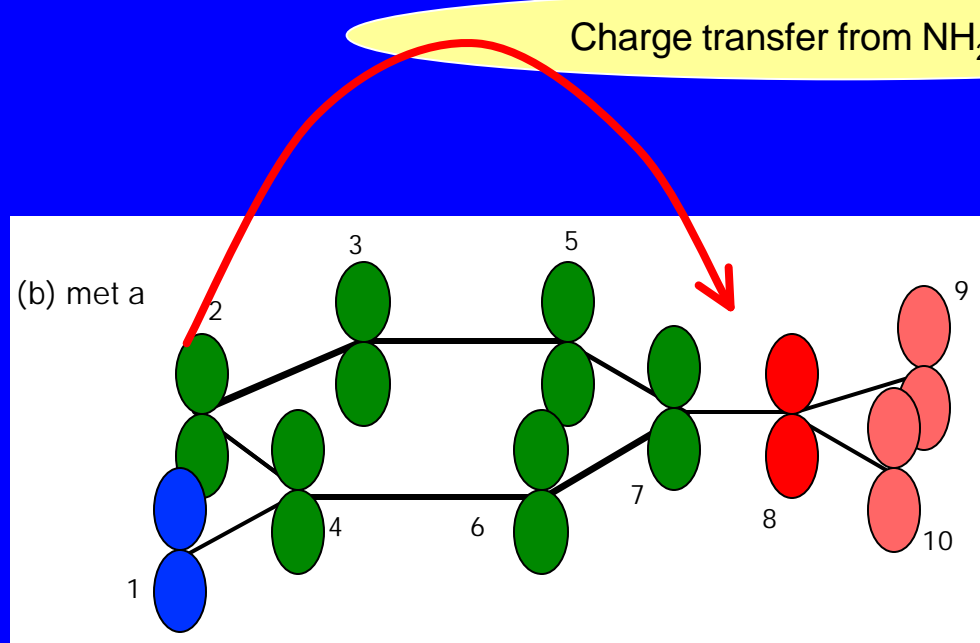
- Wavevector dependence of Stationary resonant x-ray emission spectra



Summary

- Dynamics of relative electron-hole motion of core-exciton can be probed
- Excitation to a localized core exciton ? weak time dependence
x-ray emission becomes an atomic event
- Excitation to a delocalized state ? strong time dependence
periodic relative motion of core exciton
- strong wavevector dependence ? detect entire valence exciton band

8. X-ray four-wave-mixing in nitroaniline



- Model Hamiltonian

$$\hat{H}_{tot} = \hat{H}_v + \hat{H}_e + \hat{U}_{ev},$$

$$\hat{H}_v = \sum_{\alpha} \sum_{\sigma} \epsilon_{\alpha} c_{\alpha\sigma}^{\dagger} c_{\alpha\sigma} + \frac{1}{2} \sum_{\alpha_1\alpha_2\alpha_3\alpha_4} \sum_{\sigma\sigma'} u_v(\alpha_1\alpha_2; \alpha_3\alpha_4) c_{\alpha_1\sigma}^{\dagger} c_{\alpha_2\sigma'}^{\dagger} c_{\alpha_3\sigma'} c_{\alpha_4\sigma},$$

$$\hat{H}_e = \sum_{\underline{l}=\underline{1,8}} a_{\underline{l}\sigma}^{\dagger} a_{\underline{l}\sigma} + \frac{1}{2} \sum_{\underline{l,m}=\underline{1,8}} \sum_{\sigma\sigma'} u_e(\underline{l}; \underline{m}) a_{\underline{l}\sigma}^{\dagger} a_{\underline{m}\sigma'}^{\dagger} a_{\underline{m}\sigma'} a_{\underline{l}\sigma},$$

$$\hat{U}_{ev} = - \sum_{\underline{l}=\underline{1,8}} \sum_{\alpha_1\alpha_2} \sum_{\sigma\sigma'} u_{ev}(\alpha_1; \alpha_2) (1 - a_{\underline{l}\sigma}^{\dagger} a_{\underline{l}\sigma}) c_{\alpha_1\sigma}^{\dagger} c_{\alpha_2\sigma'}.$$

Ground state

$$|g\rangle = a_{\underline{1}\uparrow}^{\dagger} a_{\underline{1}\downarrow}^{\dagger} a_{\underline{8}\uparrow}^{\dagger} a_{\underline{8}\downarrow}^{\dagger} |vac\rangle .$$

Single-core-excited state basis

$$|\underline{1}; \alpha\rangle = \frac{1}{2} (a_{\underline{1}\uparrow} c_{\alpha\uparrow}^{\dagger} + a_{\underline{1}\downarrow} c_{\alpha\downarrow}^{\dagger}) |g\rangle \quad \text{N 1s (NH2) excitation}$$

$$|\underline{8}; \alpha\rangle = \frac{1}{2} (a_{\underline{8}\uparrow} c_{\alpha\uparrow}^{\dagger} + a_{\underline{8}\downarrow} c_{\alpha\downarrow}^{\dagger}) |g\rangle, \quad \text{N 1s (NO2) excitation}$$

Double-core-excited state basis

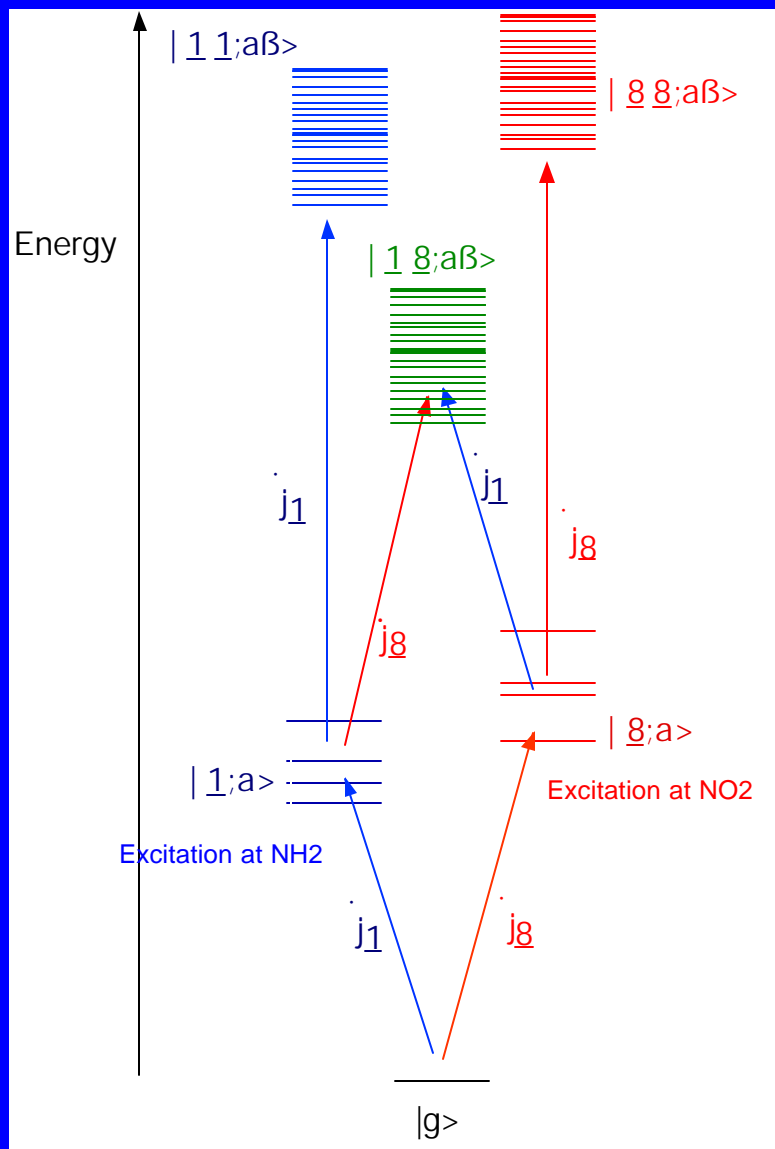
$$|\underline{1}, \underline{1}; \alpha, \beta\rangle = -\frac{1}{\sqrt{2}} a_{\underline{1}\uparrow} a_{\underline{1}\downarrow} (c_{\alpha\uparrow}^{\dagger} c_{\beta\downarrow}^{\dagger} - c_{\alpha\downarrow}^{\dagger} c_{\beta\uparrow}^{\dagger}) |g\rangle \quad (\alpha < \beta)$$

$$|\underline{8}, \underline{8}; \alpha, \beta\rangle = -\frac{1}{\sqrt{2}} a_{\underline{8}\uparrow} a_{\underline{8}\downarrow} (c_{\alpha\uparrow}^{\dagger} c_{\beta\downarrow}^{\dagger} - c_{\alpha\downarrow}^{\dagger} c_{\beta\uparrow}^{\dagger}) |g\rangle \quad (\alpha < \beta)$$

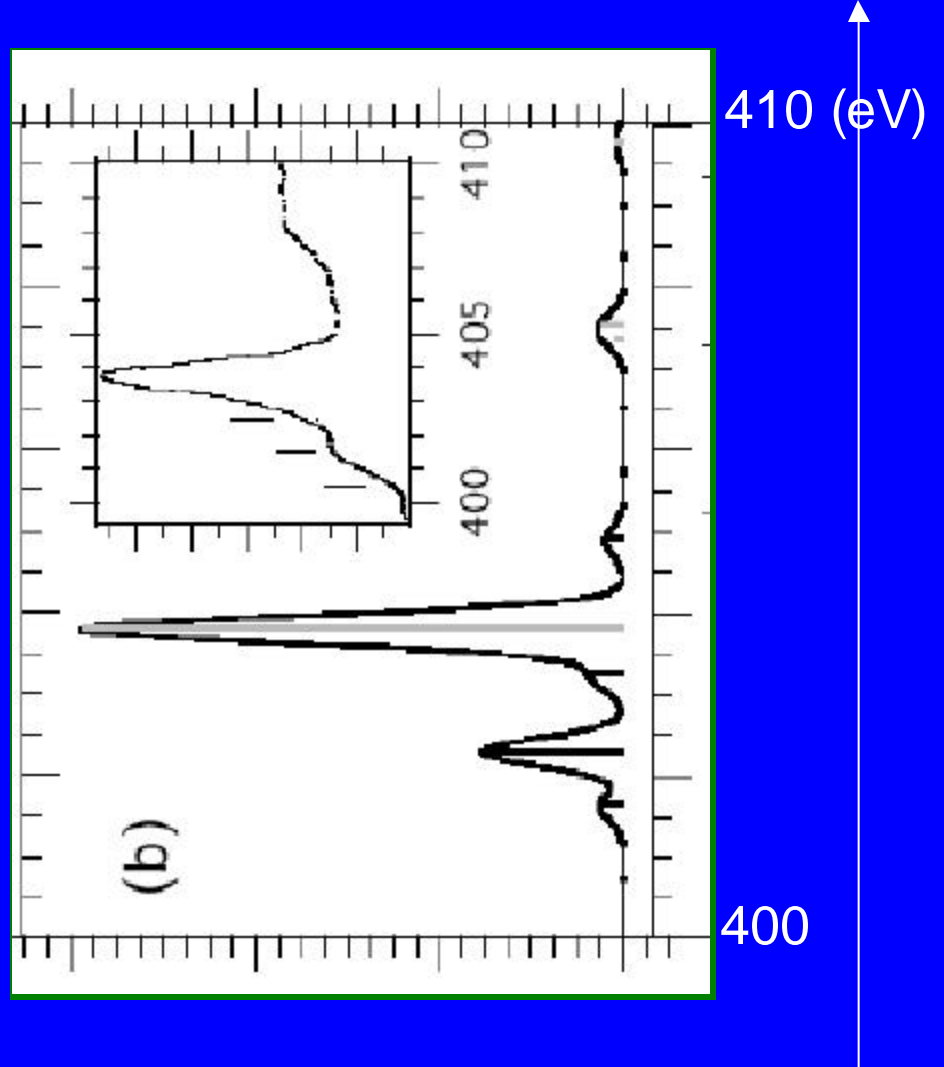
$$|\underline{1}, \underline{8}; \alpha, \beta(\text{para})\rangle = \frac{1}{\sqrt{2}} (a_{\underline{8}\uparrow} c_{\alpha\uparrow}^{\dagger} a_{\underline{1}\downarrow} c_{\beta\downarrow}^{\dagger} + a_{\underline{8}\downarrow} c_{\alpha\downarrow}^{\dagger} a_{\underline{1}\uparrow} c_{\beta\uparrow}^{\dagger}) |g\rangle \quad (\alpha < \beta)$$

$$|\underline{1}, \underline{8}; \alpha, \beta(\text{antipara})\rangle = \frac{1}{\sqrt{2}} (a_{\underline{8}\uparrow} c_{\alpha\uparrow}^{\dagger} a_{\underline{1}\downarrow} c_{\beta\uparrow}^{\dagger} + a_{\underline{8}\downarrow} c_{\alpha\downarrow}^{\dagger} a_{\underline{1}\uparrow} c_{\beta\uparrow}^{\dagger}) |g\rangle .$$

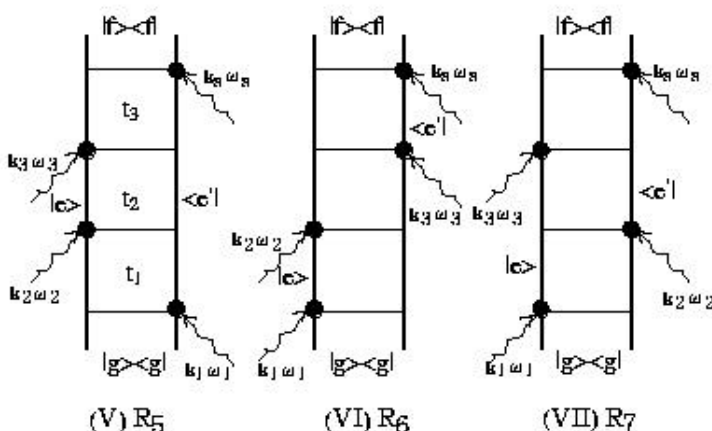
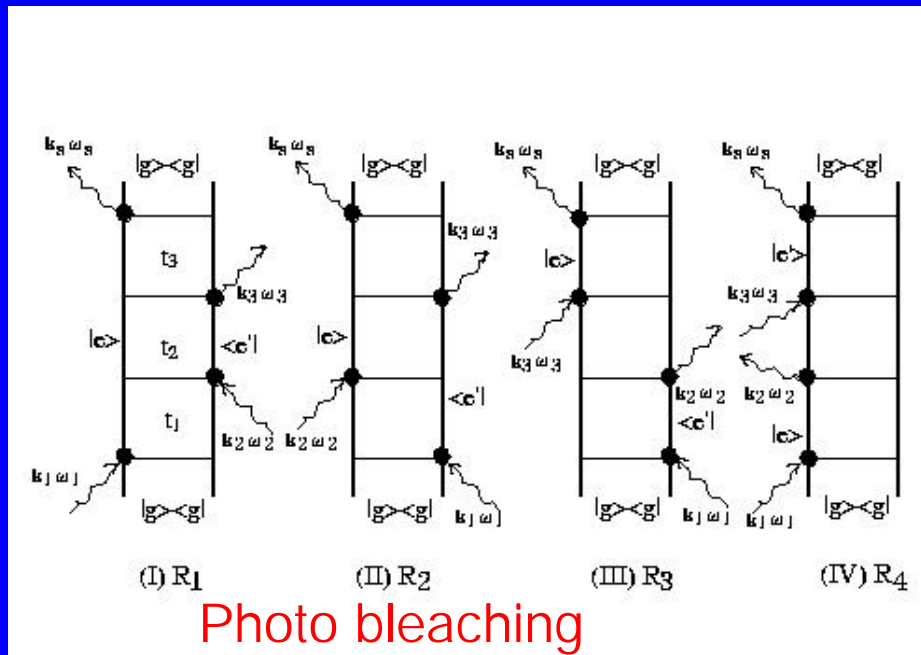
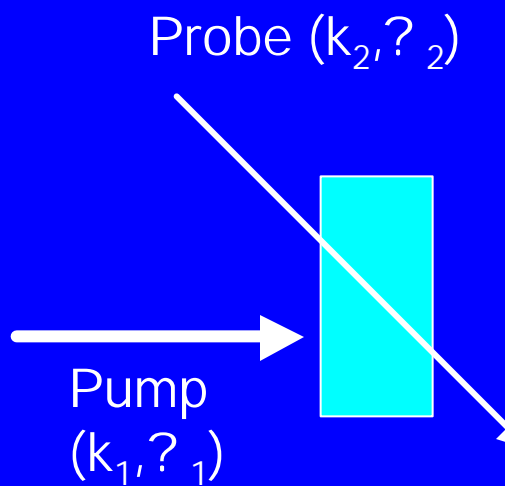
- Total level scheme



- N 1s X-ray absorption spectra



$$W_{PP}(\mathbf{k}_1, \mathbf{w}_1, \mathbf{k}_2, \mathbf{w}_2) = \text{Im} C^{(3)}(-\mathbf{k}_2, -\mathbf{w}_2; \mathbf{k}_1, \mathbf{w}_1, -\mathbf{k}_1, -\mathbf{w}_1, \mathbf{k}_2, \mathbf{w}_2)$$

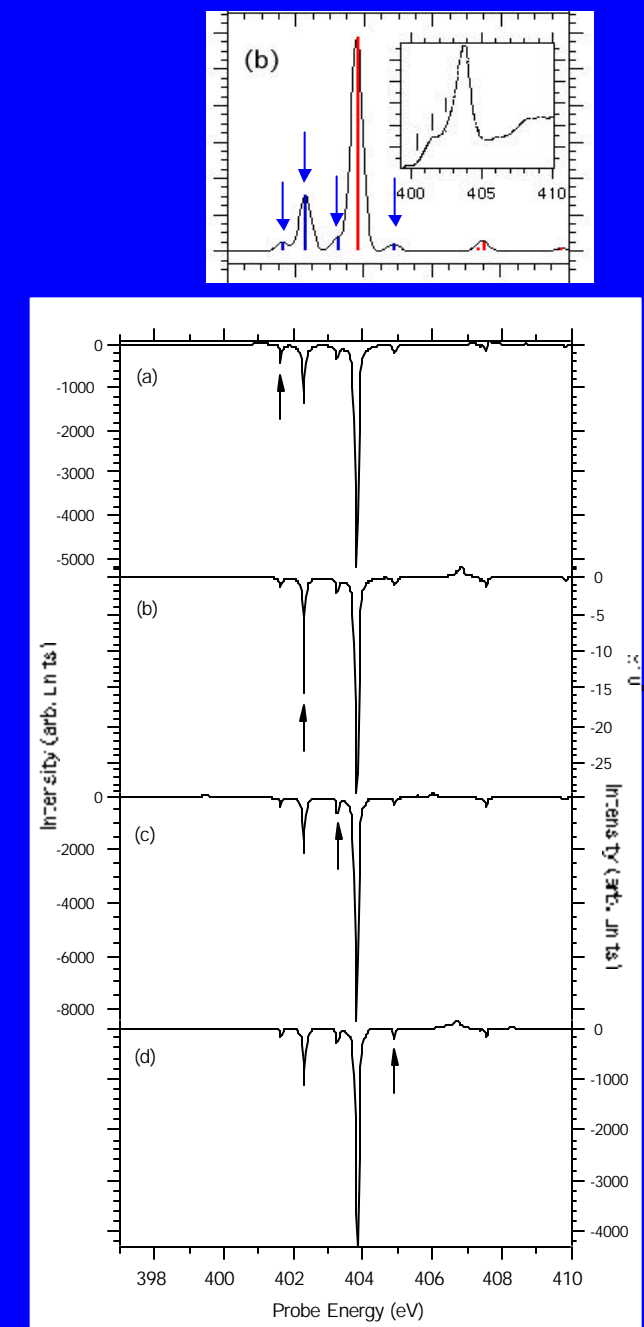
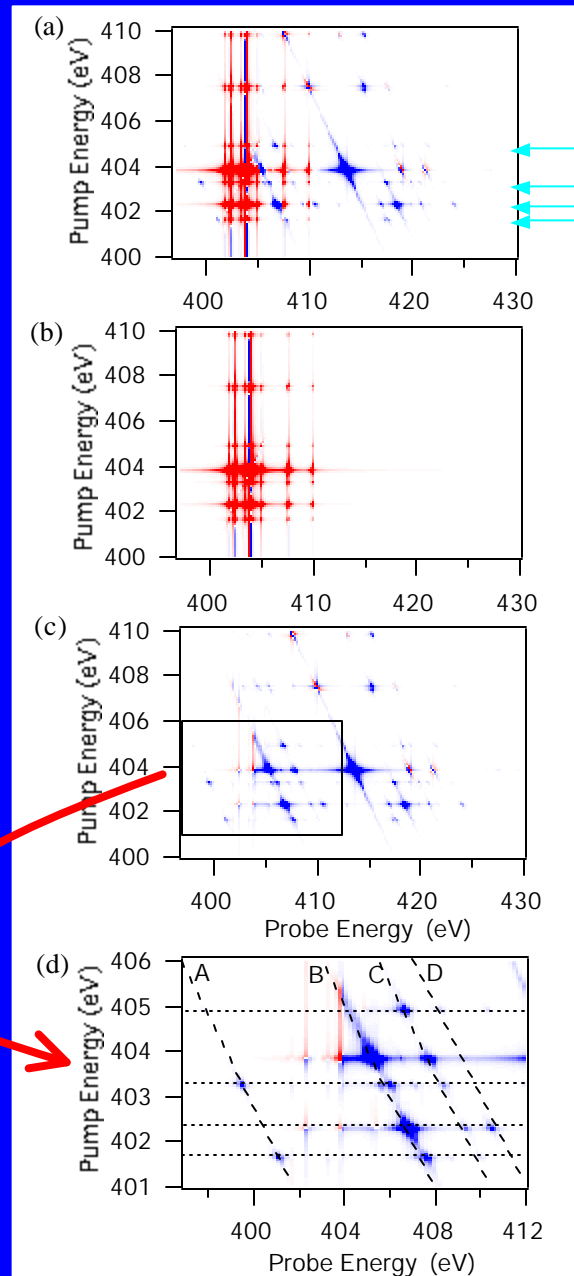


Excited state absorption

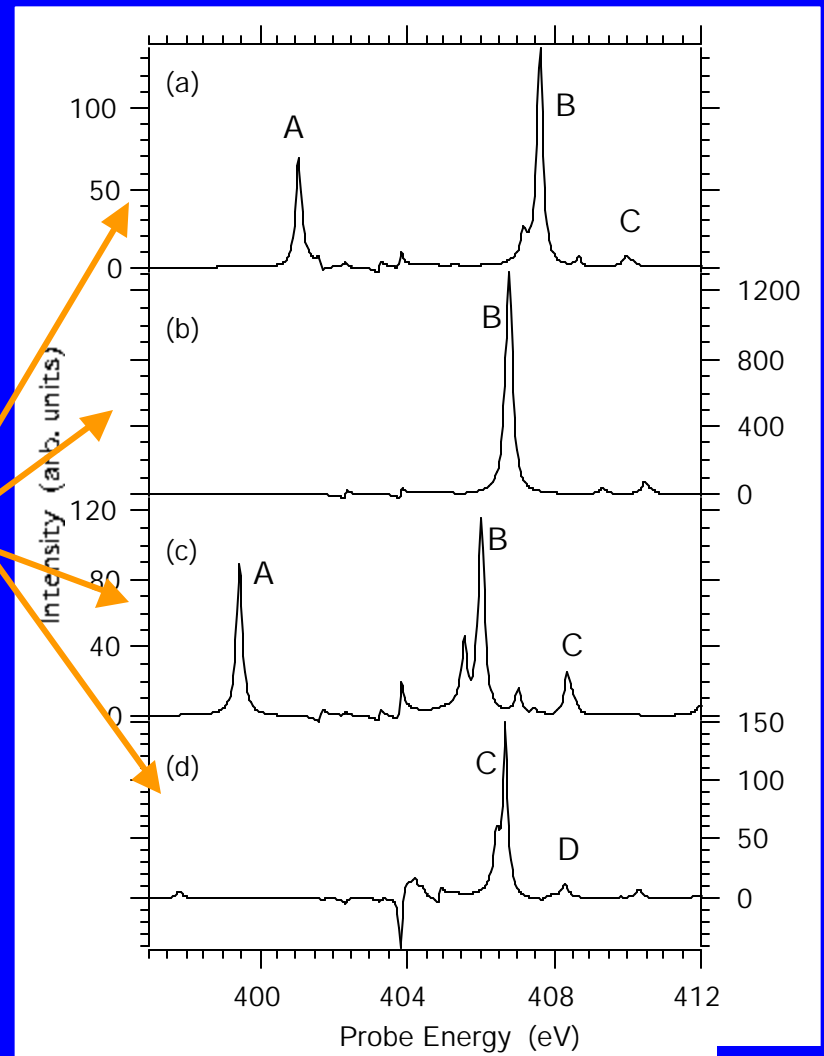
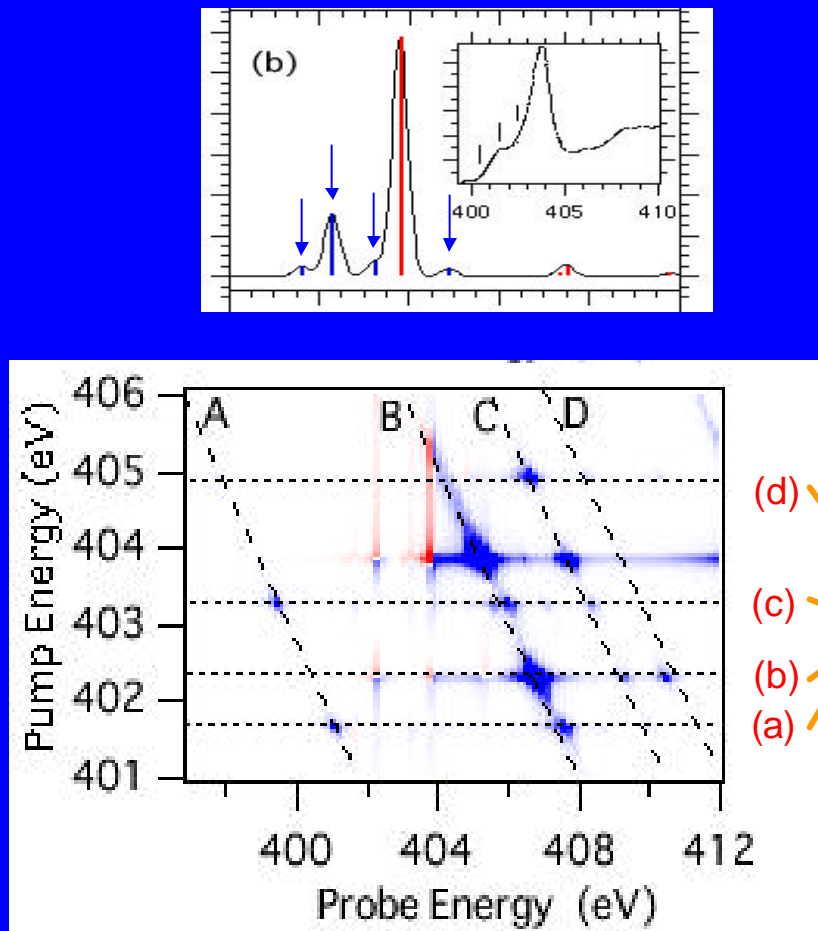
Fig.13

- N 1s X-ray pump-probe spectra

PB component
ESA component



N 1s (NH₂) pump & probe spectra: ESA component

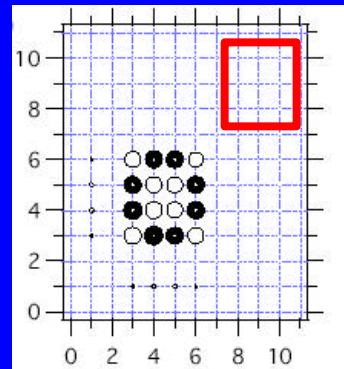


Correlation between pump and probe:

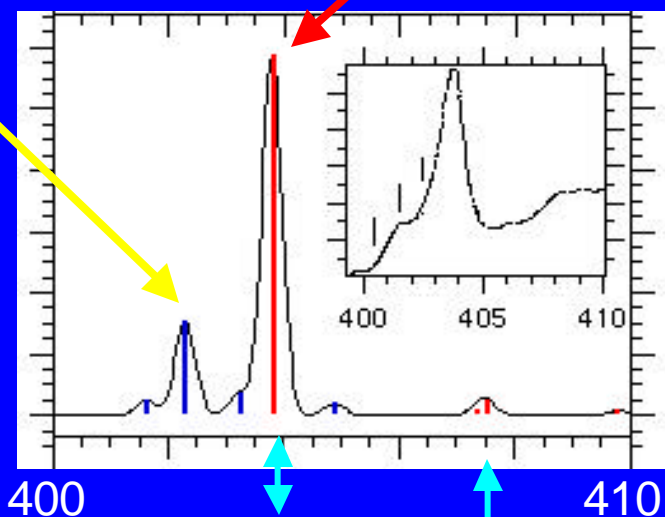
$$\hbar\mathbf{w}_1 + \hbar\mathbf{w}_2 + E_{Ground} = E_{Final}$$

- Density matrix in the core-excited states

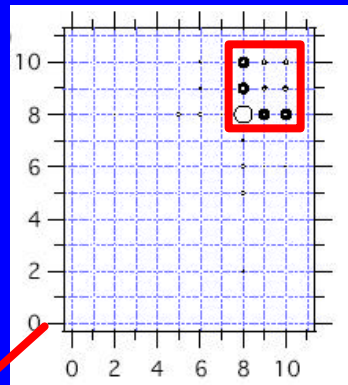
$$\rho_{\underline{L},nm}^{\xi} \equiv \sum_{\sigma\sigma'} \langle \Psi_{\xi} | c_{m\sigma}^{\dagger} c_{n\sigma'} a_{\underline{L}\sigma}^{\dagger} a_{\underline{L}\sigma} | \Psi_{\xi} \rangle,$$



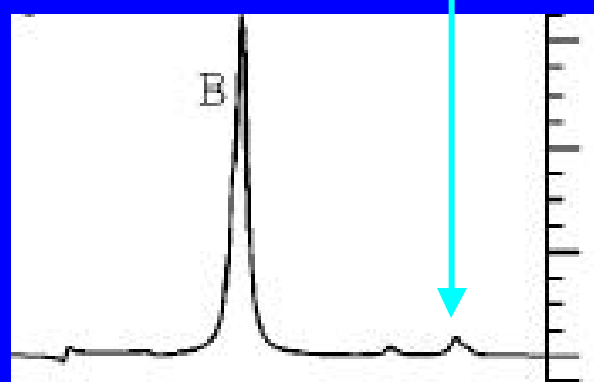
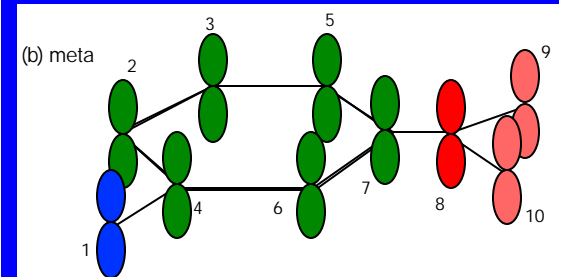
Localized in benzene ring



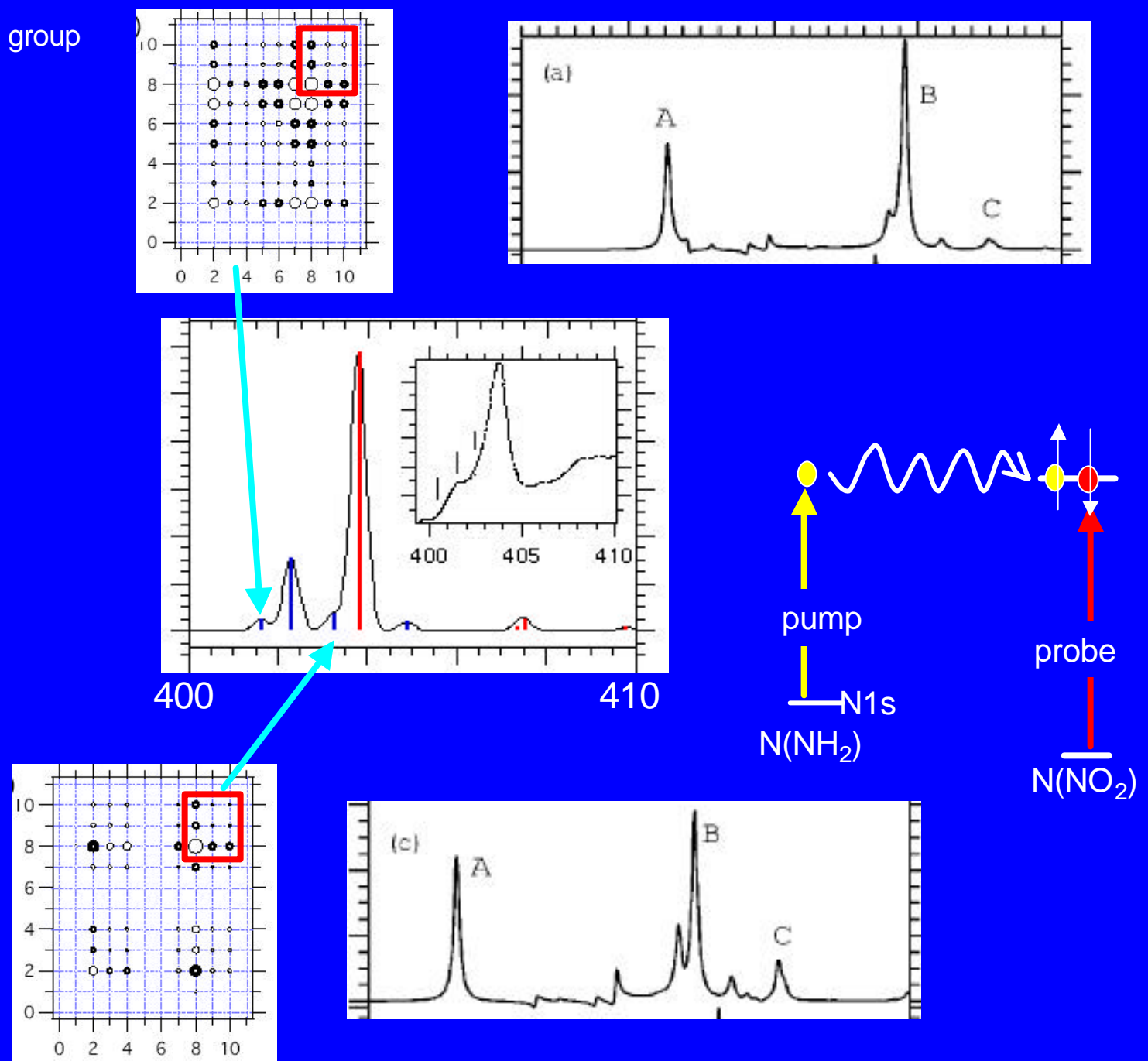
Pump-probe absorption



N 1s core exciton strongly localized in NO₂



Extended to NO₂ group



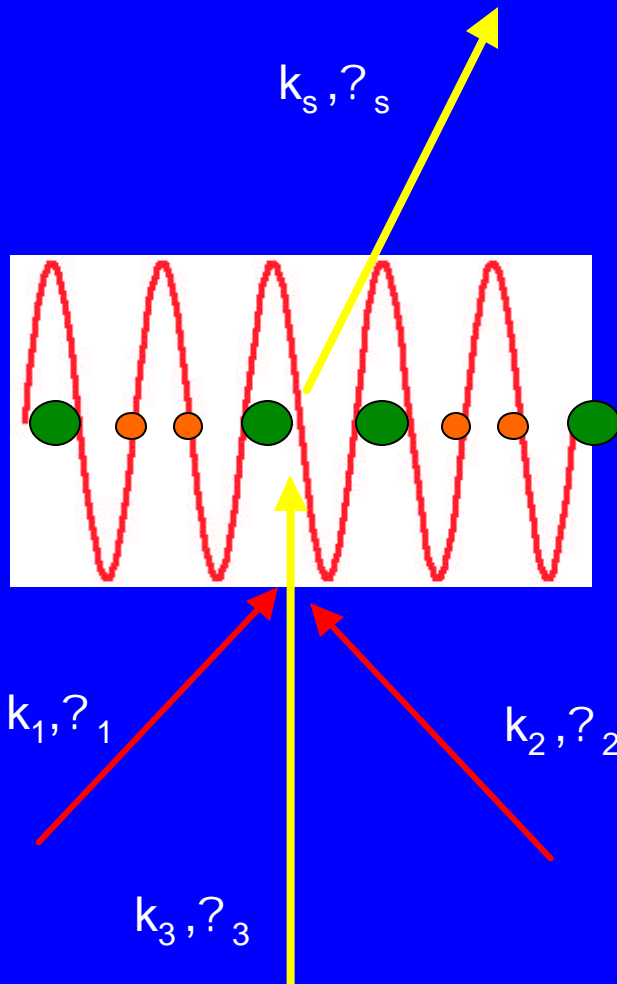
Summary

- spatial coherence between different sites can be detected
(in core excited states)

BY N 1s x-ray pump-probe spectroscopy:

1. excited electron is localized around benzene ring
? probe absorption is unaffected ? N 1s (NO_2) absorption
2. excited electron is delocalized
? probe absorption is strongly affected

9. Coherent X-ray Raman Scattering in 1D molecular chain

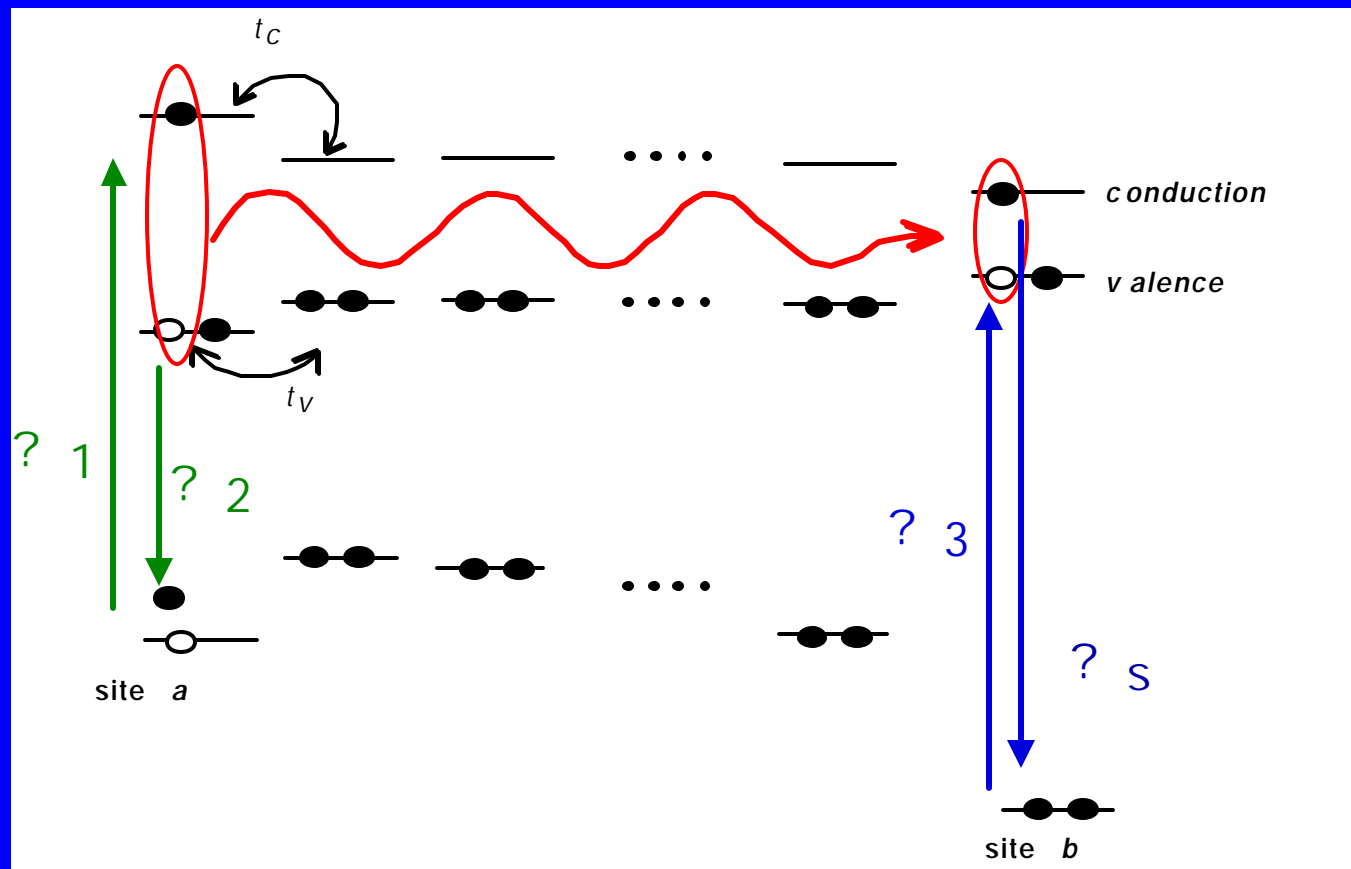


Signal x-ray beam
 $k_s = k_1 - k_2 + k_3, \omega_s = \omega_1 - \omega_2 + \omega_3$

$\omega_1 - \omega_2$ = valence excitation energy
 $q = k_1 - k_2$: grating vector

Condition of detecting spatial coherence between different atomic sites

- i) $\omega_1 - \omega_2$ = valence excitation
- ii) ω_1, ω_2 tuned to a core resonance of site a
- iii) ω_3, ω_s tuned to the core resonance of site b



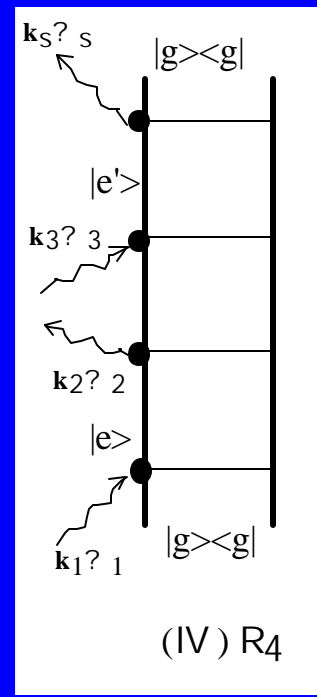
- Hamiltonian

$$\begin{aligned}
 H = & -\sum_{l=0}^{N-1} \mathbf{e}_{core} a_l^\dagger a_l + \sum_{l=0}^{N-1} \mathbf{e}_{val} v_l^\dagger v_l - \sum_{l=0}^{N-1} \mathbf{e}_{cond} c_l^\dagger c_l \\
 & + \sum_{l,m=0}^{N-1} t_{lm}^{val} v_l^\dagger v_m + \sum_{l,m=0}^{N-1} t_{lm}^{cond} c_l^\dagger c_m \\
 & - \sum_{l,l',m,m'} U_{l'm';lm}^{core-cond} c_{l'}^\dagger a_{m'}^\dagger a_m c_l - \sum_{l,l',m,m'} U_{l'm' \neq m}^{val-cond} c_{l'}^\dagger v_{m'}^\dagger v_m c_l \\
 & + \sum_{l,l',m,m'} U_{l'm';lm}^{core-core} a_{l'}^\dagger a_{m'}^\dagger a_m a_l + \sum_{l,l',m,m'} U_{l'm' \neq m}^{cond-cond} c_{l'}^\dagger c_{m'}^\dagger c_m c_l
 \end{aligned}$$

Core-core

Condction-conduction

Effective diagram



- Expression of signal

Homodyne detection:

$$I_{\text{homo}} = |\mathbf{c}^{(3)}|^2$$

Heterodyne detection:

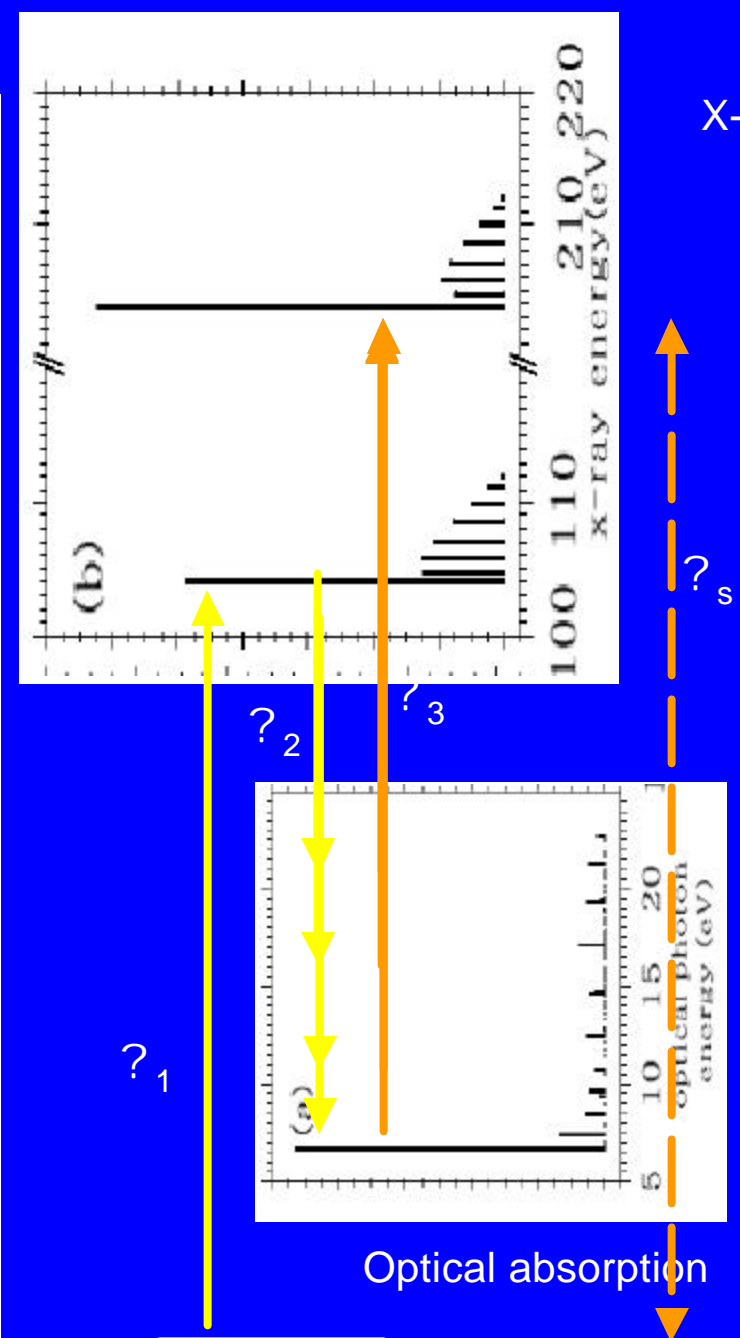
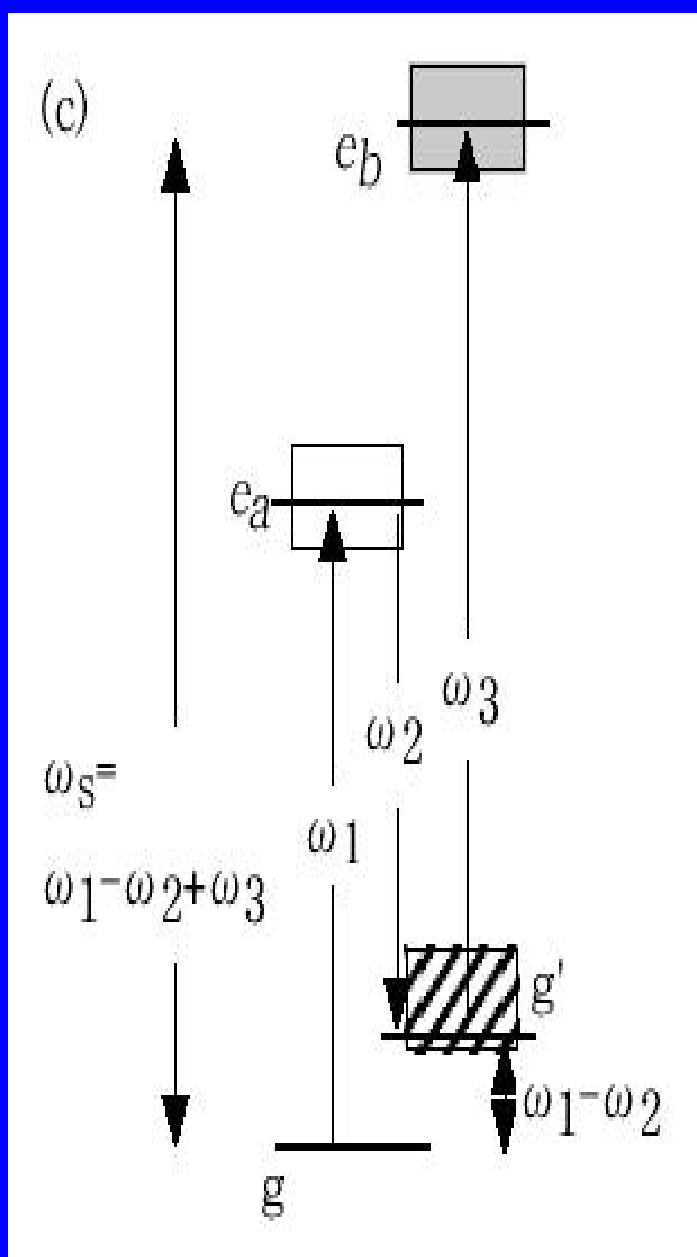
$$I_{\text{hetero}} = \text{Re } \mathbf{c}^{(3)}, \text{ Im } \mathbf{c}^{(3)}$$

$$\mathbf{c}^{(3)} = R_{IV} = \sum_{g'} \mathbf{a}_{g,g'}(\mathbf{w}_1, \mathbf{w}_s) \frac{1}{\mathbf{w}_1 - \mathbf{w}_2 - \mathbf{w}_{g',g} + i\Gamma_{g',g}}$$

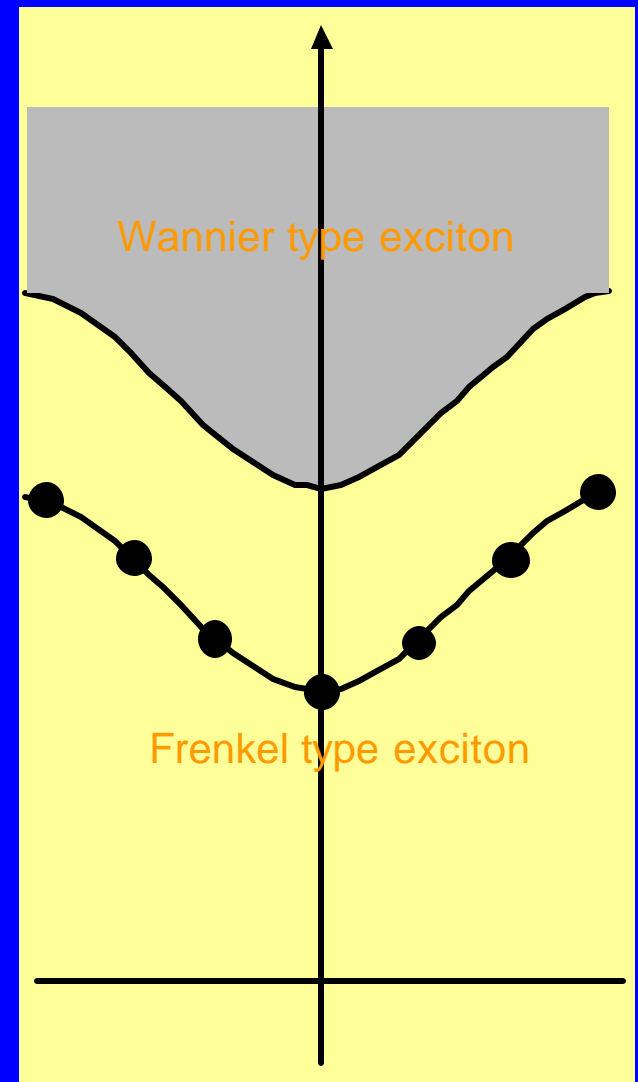
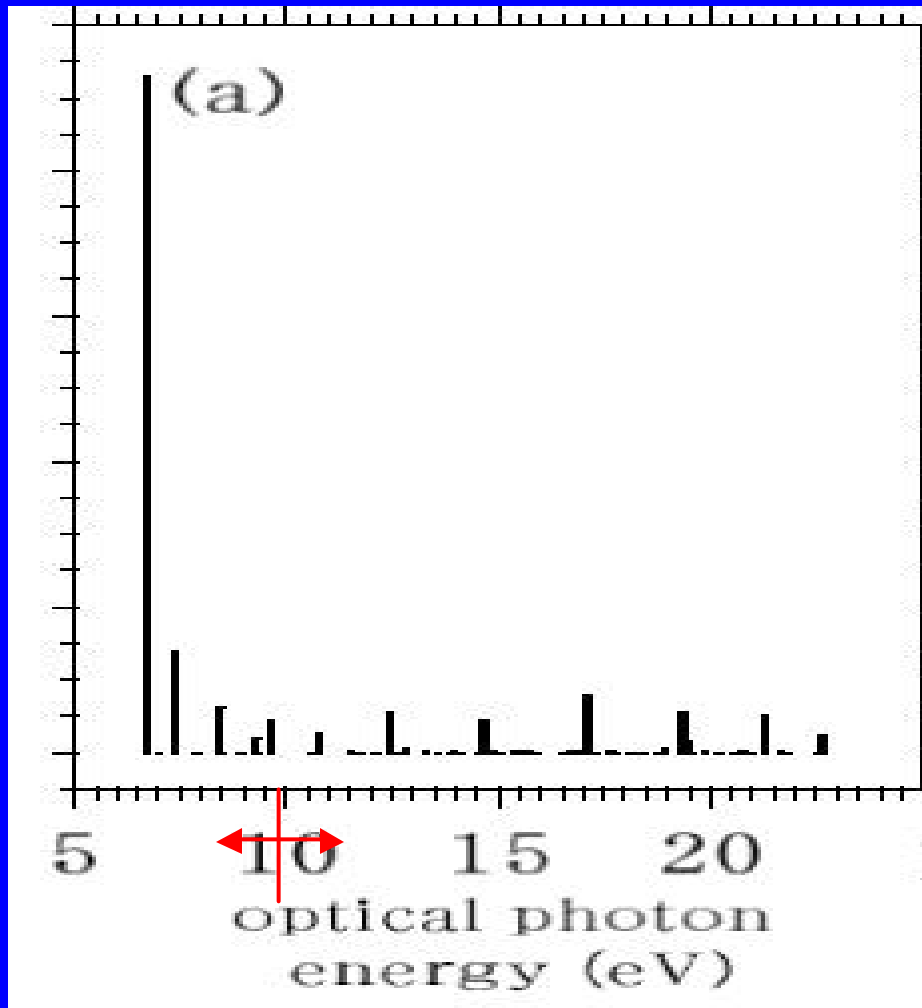
$$\mathbf{a}_{g,g'}(\mathbf{w}_1, \mathbf{w}_s) = \sum_{m,n} \sum_{e_m, e_n} \exp[i\mathbf{q} \cdot (\mathbf{R}_n - \mathbf{R}_m)] \cdot \frac{j_{g,e_m} j_{e_m g'}}{\mathbf{w}_s - \mathbf{w}_{e_m,g} + i\Gamma_{e_m,g}} \cdot \frac{j_{g',e_n} j_{e_n,g}}{\mathbf{w}_1 - \mathbf{w}_{e_n,g} + i\Gamma_{e_n,g}}$$

Detected at site m

Polarization induced at site n

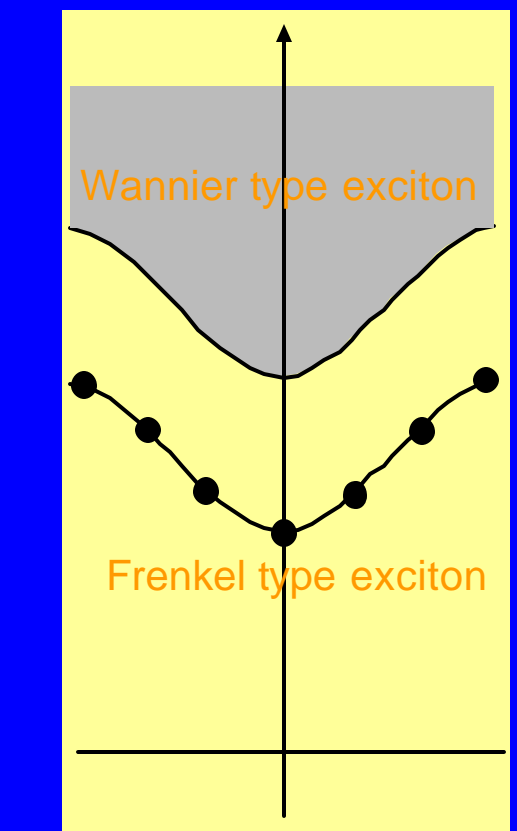
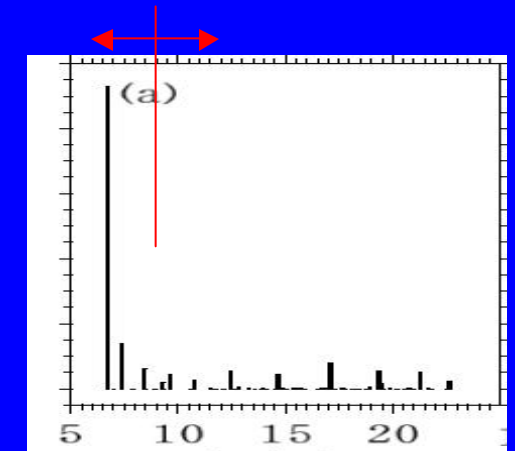
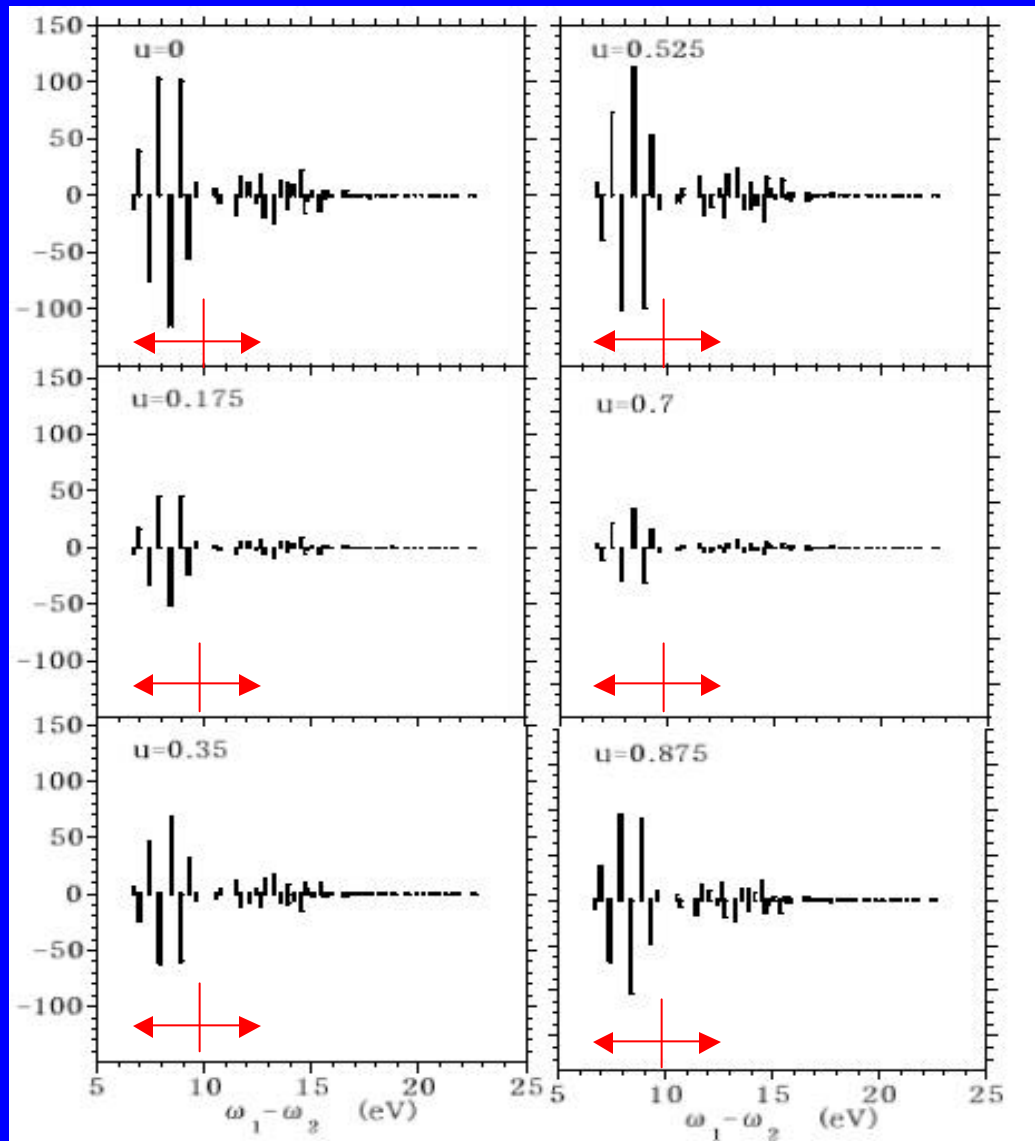


- Valence exciton state, optical absorption spectrum

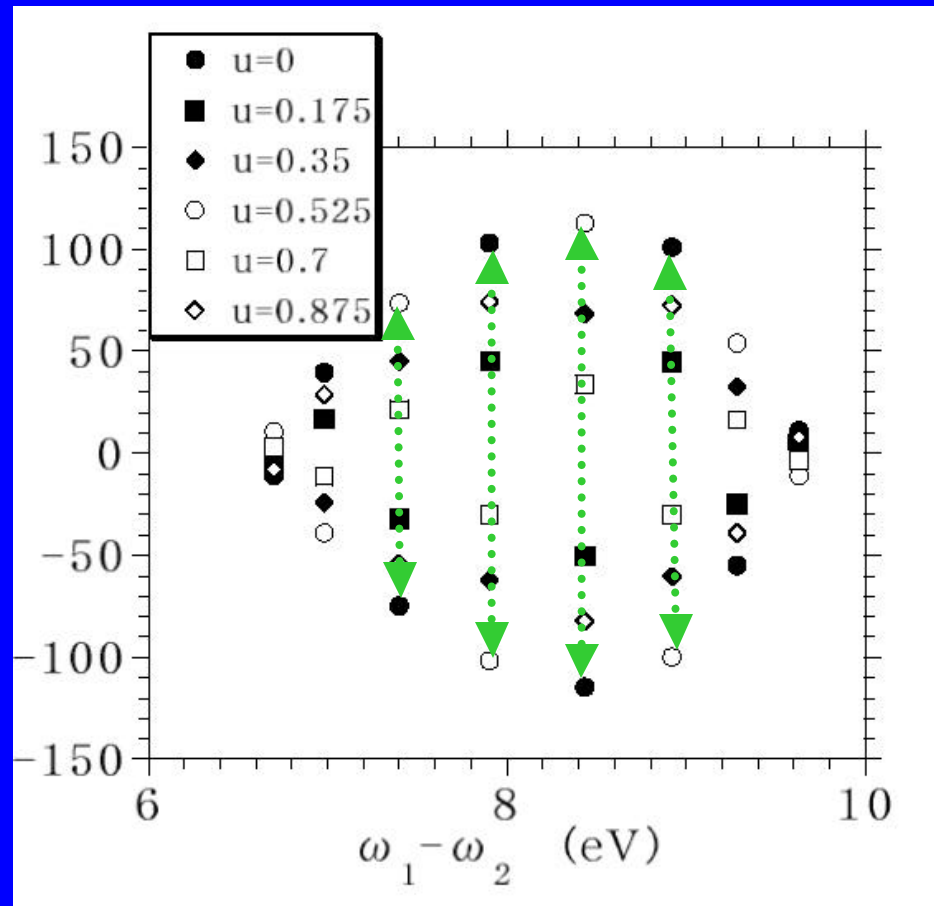


- Heterodyne CXRS for various scattering wavevectors

$\text{Im } \mathbf{c}^{(3)}$



- Wavevector dependence of Frenkel exciton peak intensities

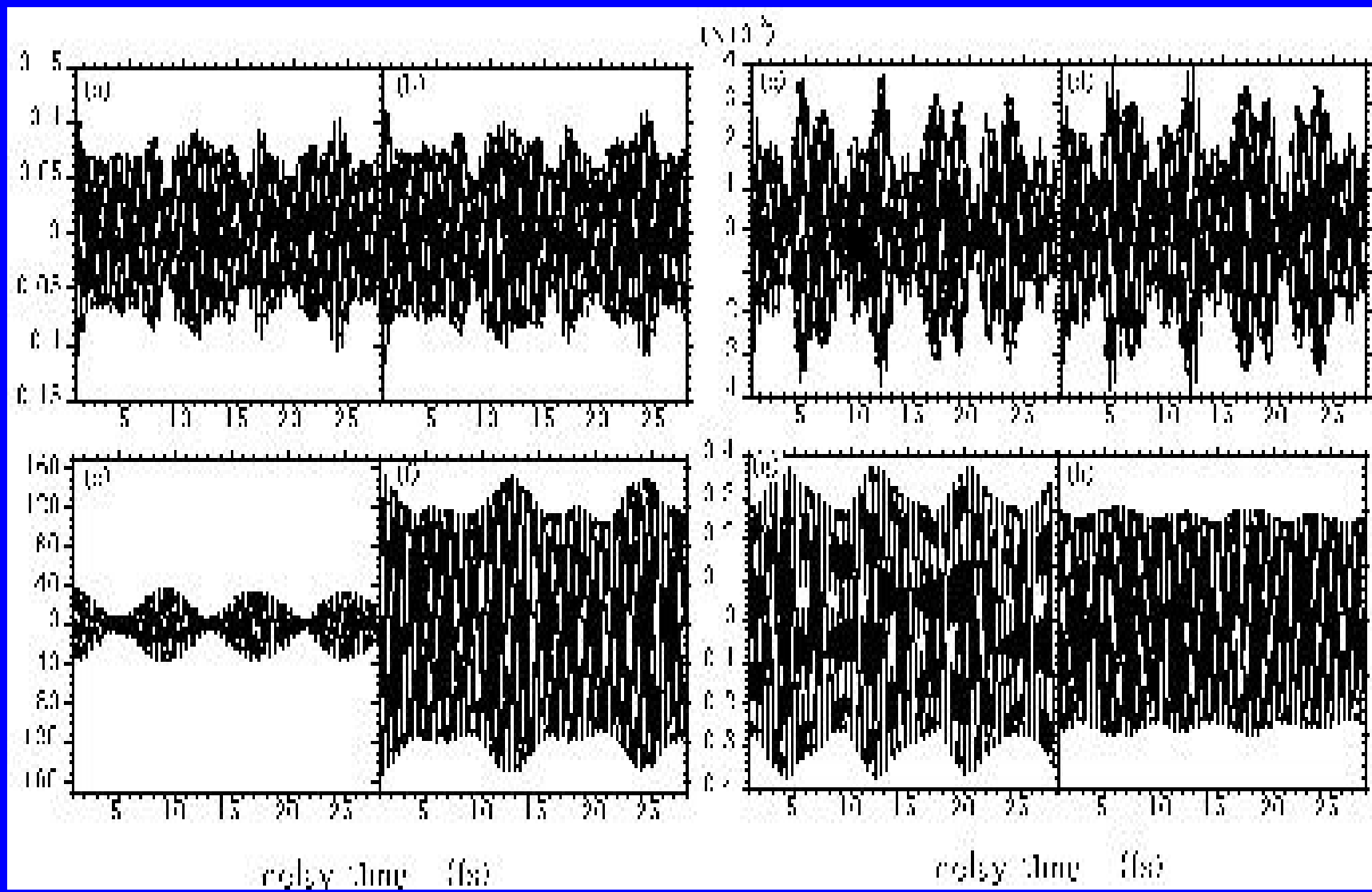


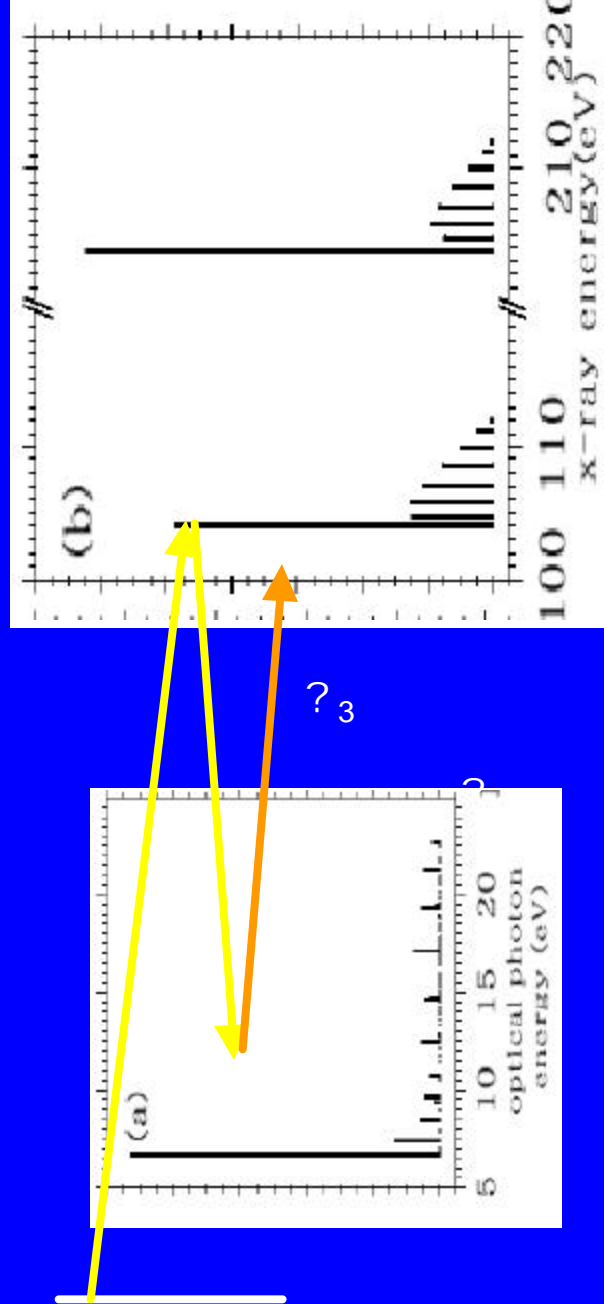
$$u = q/2pL$$

Strong q dependence:
Exciton state is coherently delocalized over sites a and b

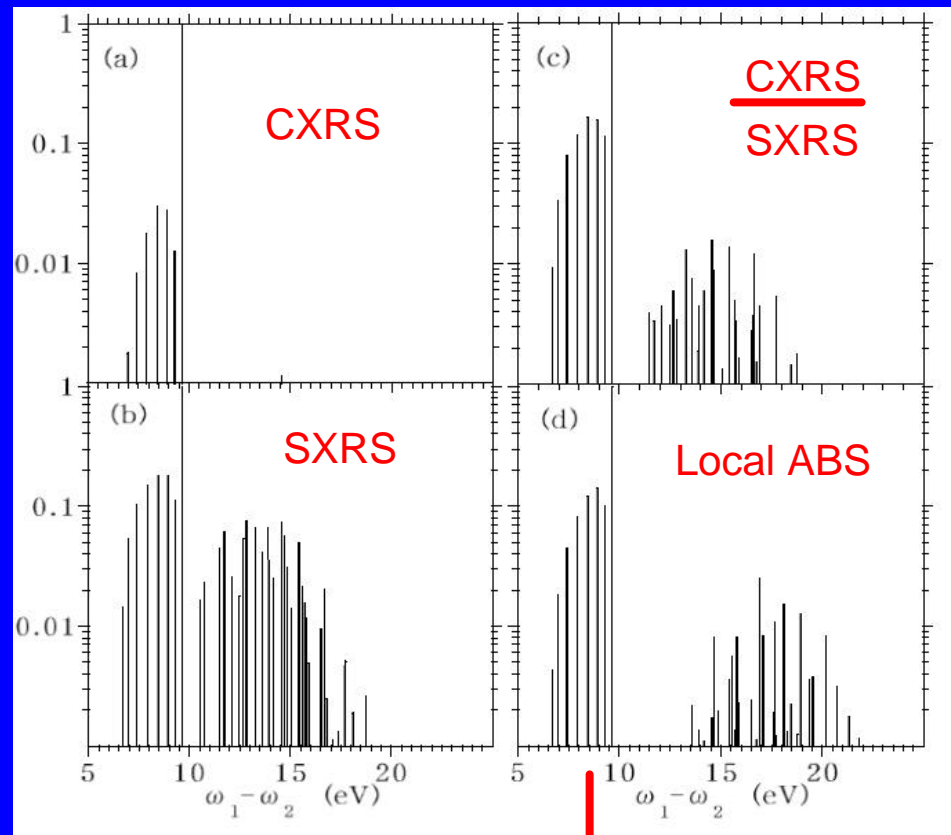
Conclusion:

- time-resolved x-ray emission spectrum
core exciton dynamics (relative motion)
- stationary x-ray pump-probe spectrum
spatial coherence of core excited states
- Coherent x-ray Raman scattering
spatial coherence of valence exciton states
- time-resolved coherent x-ray Raman scattering
valence exciton dynamics



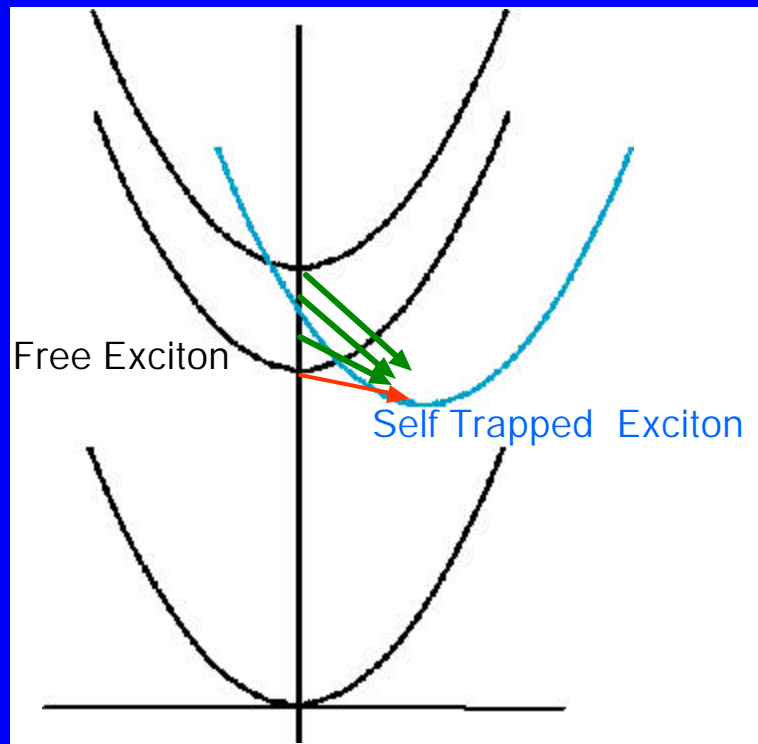


- Detection of local excitation



$$\propto \langle g' | c_a^\dagger v_a | g \rangle^2$$

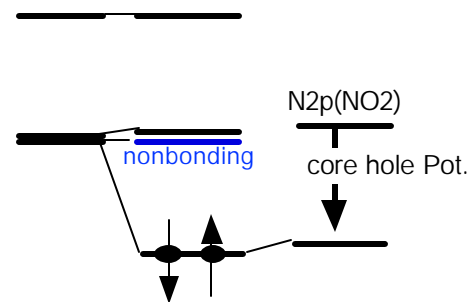
Exciton Polaron self-trapping process



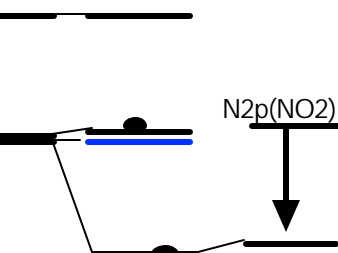
Resonant x-ray emission & Resonant Auger emission

(a)&(c)-excitation

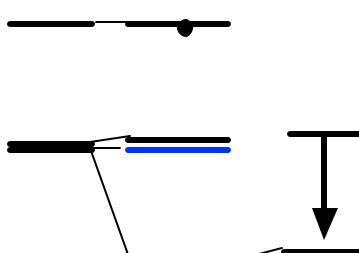
A



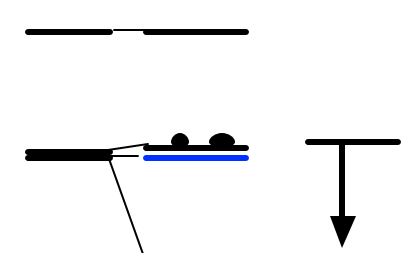
B



C

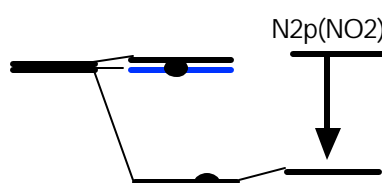


C

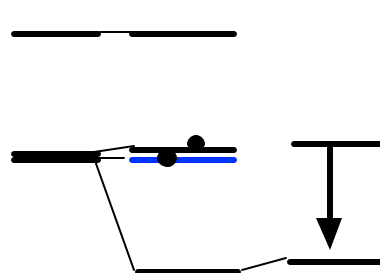


(b)-excitation

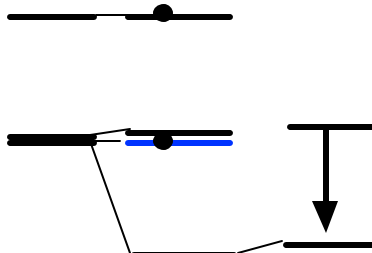
B



C

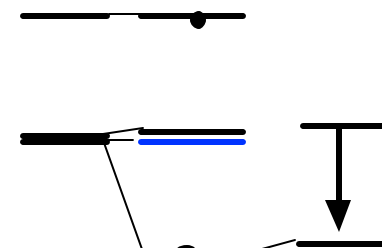


D

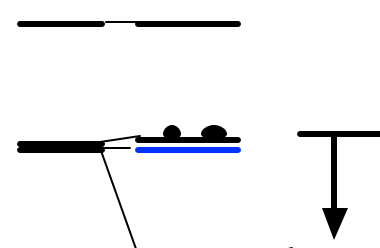


(d)-excitation

C



C



D

